NRC NATURAL ANALOG RESEARCH PROGRAM

PRESENTED BEFORE THE NWTRB, RENO, NEVADA

APRIL 16, 1991

PREPARED BY:

DR. LINDA A. KOVACH

DR. GEORGE F. BIRCHARD

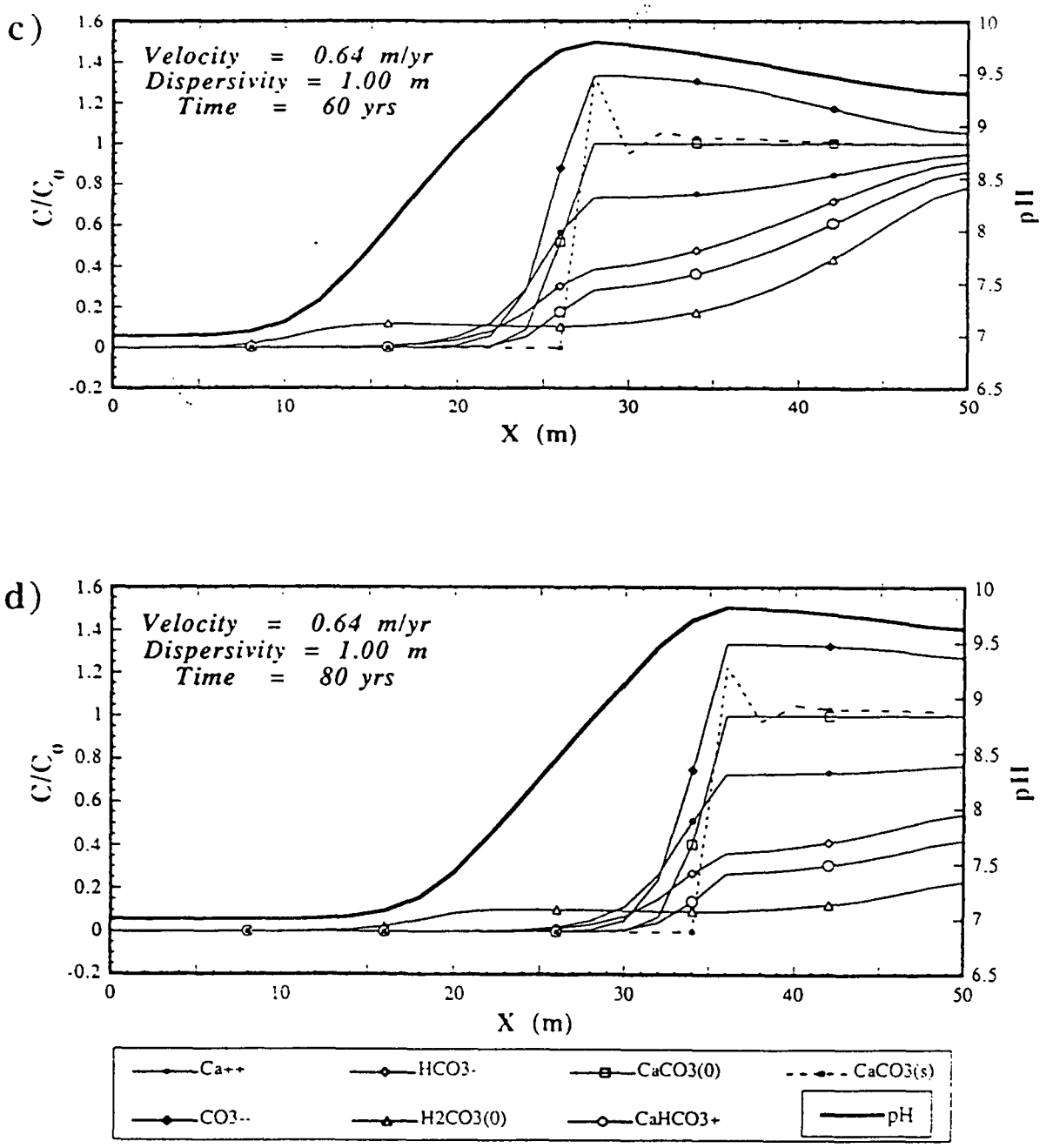

FIGURE 8 c,d – Results from a reactive solute transport simulation at 60 (c) and 80 (d) years. Concentrations are plotted relative to initial values (left axis). Variations in pH are shown by the heavy line (right axis).

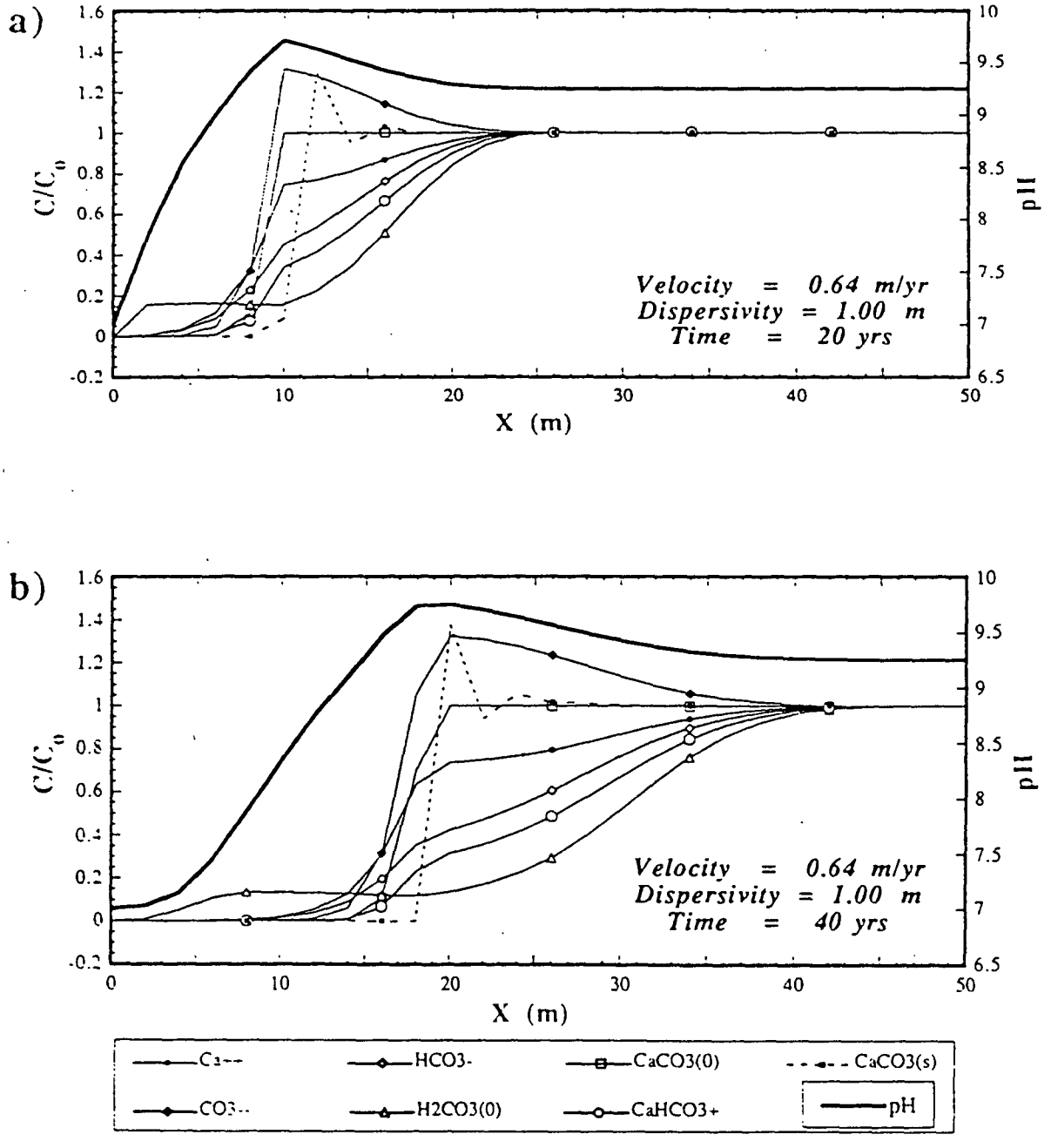

FIGURE 8 a,b – Results from a reactive solute transport simulation at 20 (a) and 40 (b) years. Concentrations are plotted relative to initial values (left axis). Variations in pH are shown by the heavy line (right axis).

Temperature

FIGURE 7c

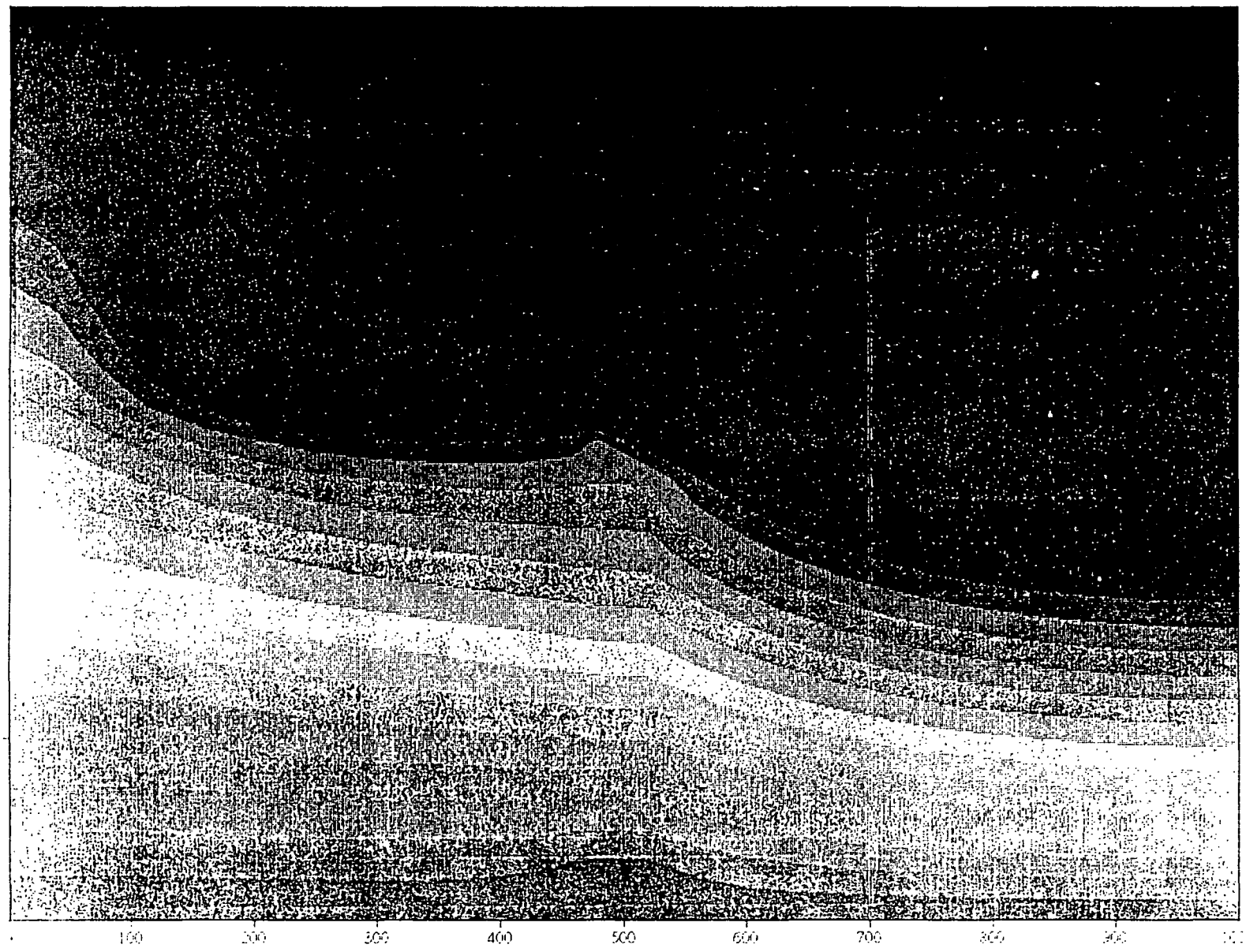

Stream Function

FIGURE 7b

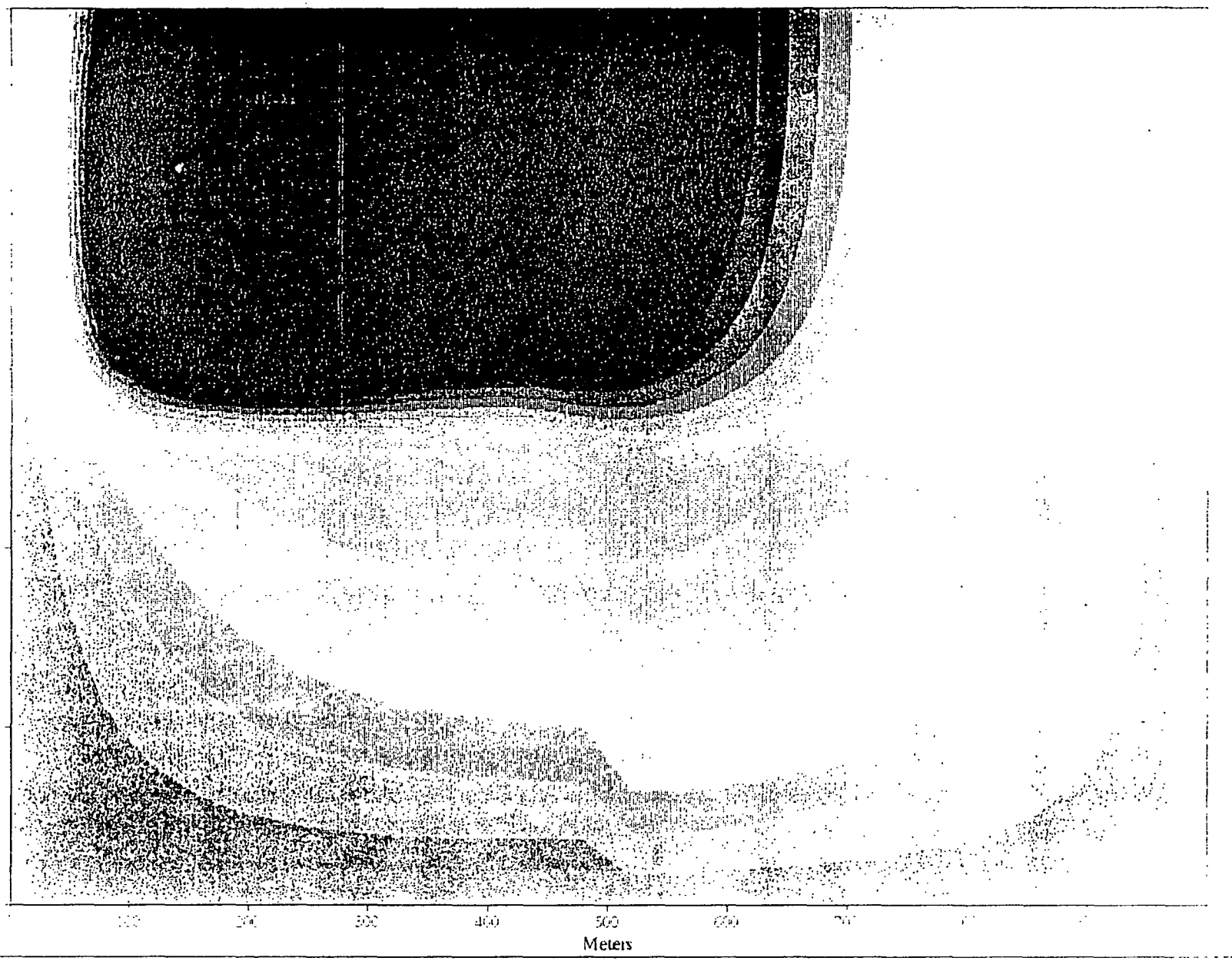

Groundwater Velocity

Vmax = 1.92 m/yr

FIGURE 7a

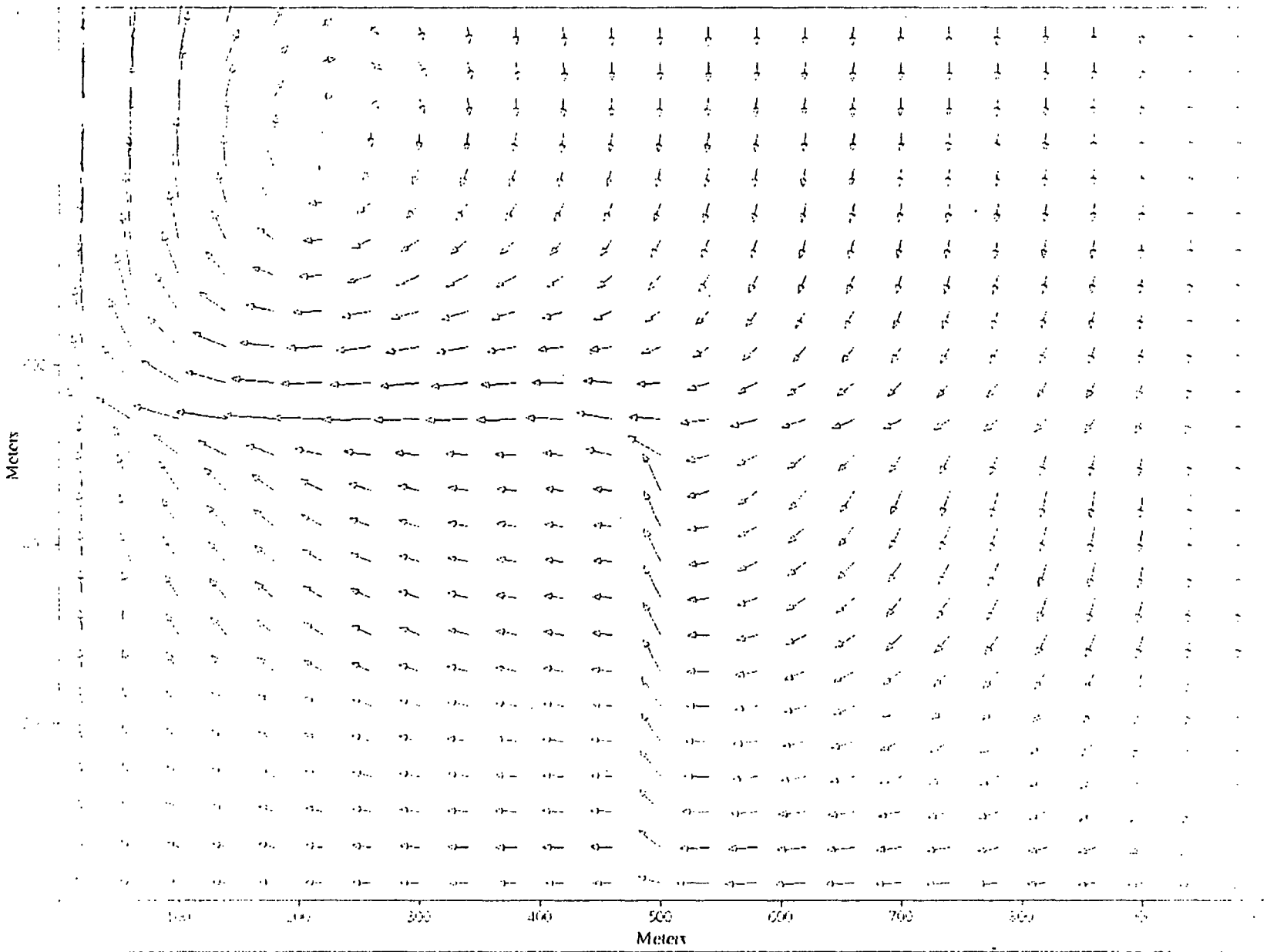

Temperature

FIGURE 6c

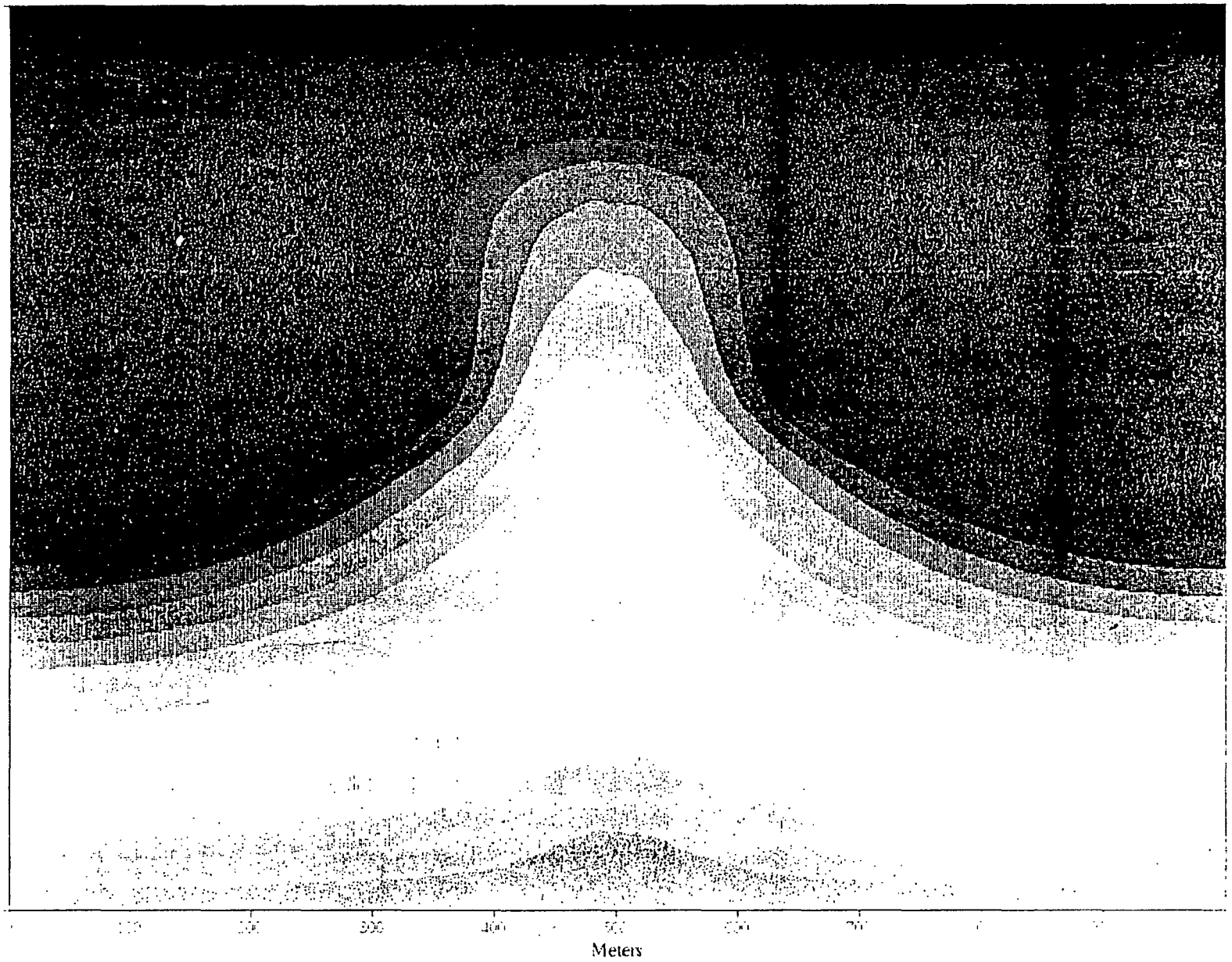

Stream Function

FIGURE 6b

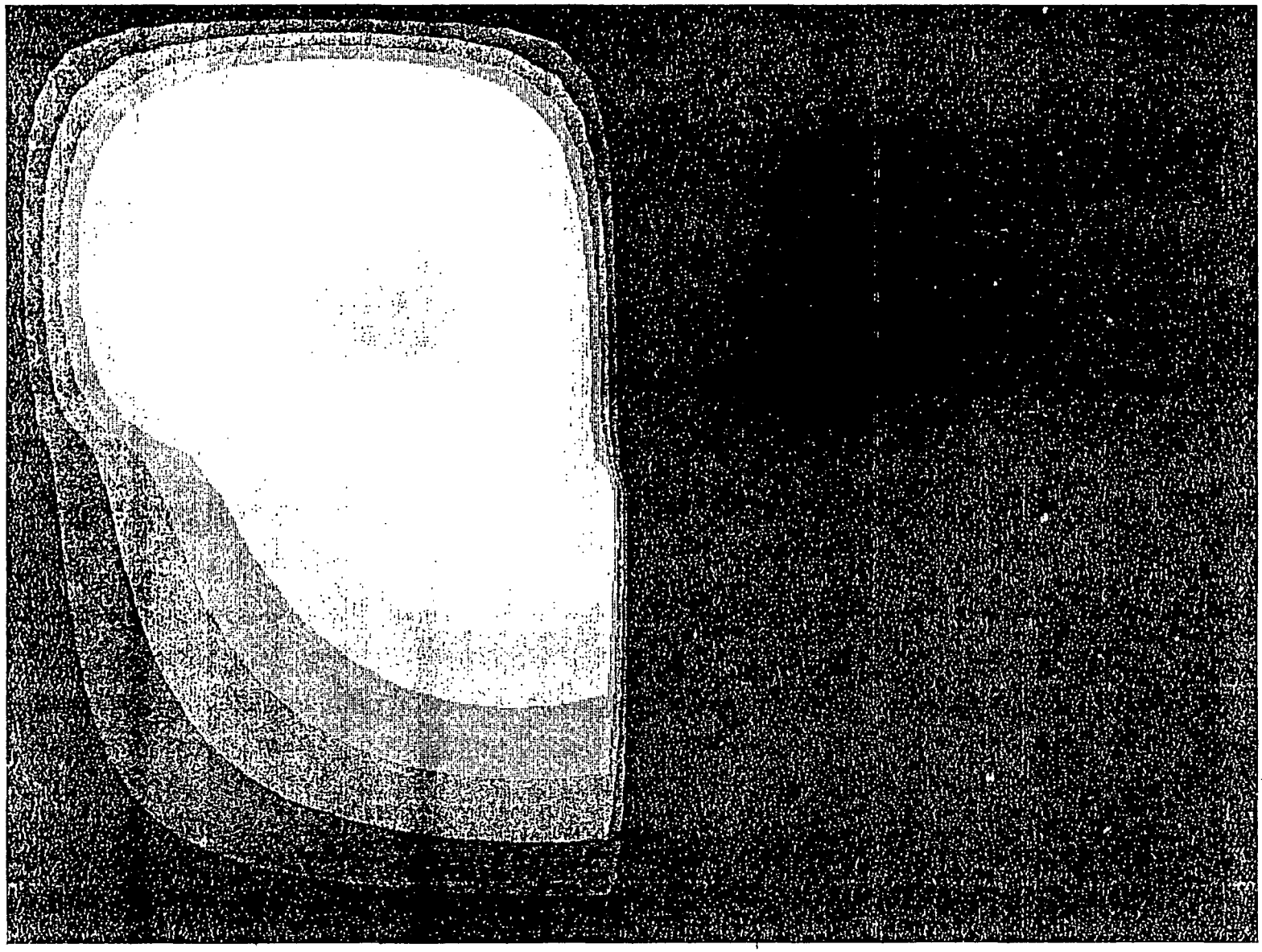

Groundwater Velocity

Vmax = 7.06 m/yr

FIGURE 6a

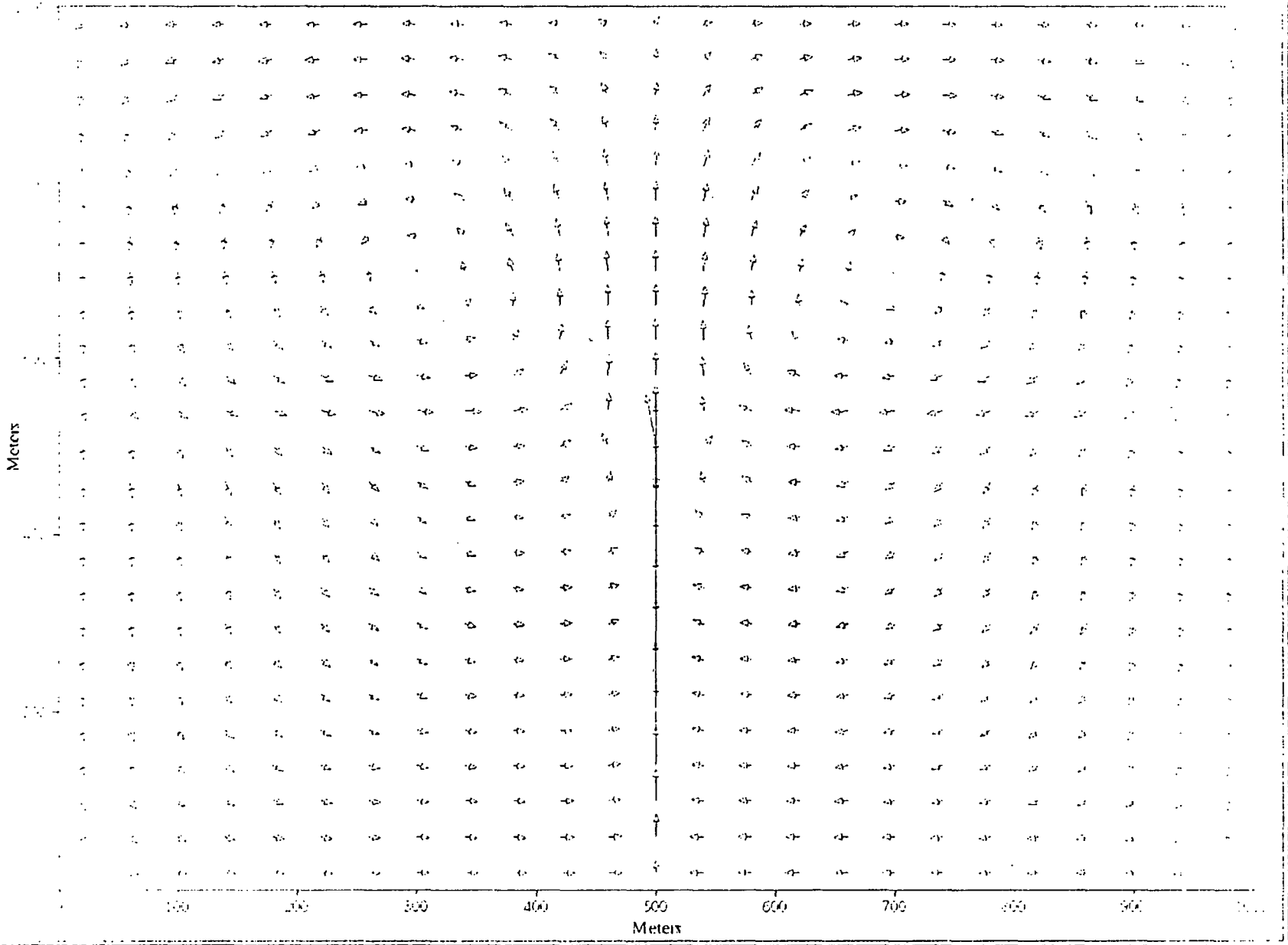

Hydrostratigraphy

FIGURE 5

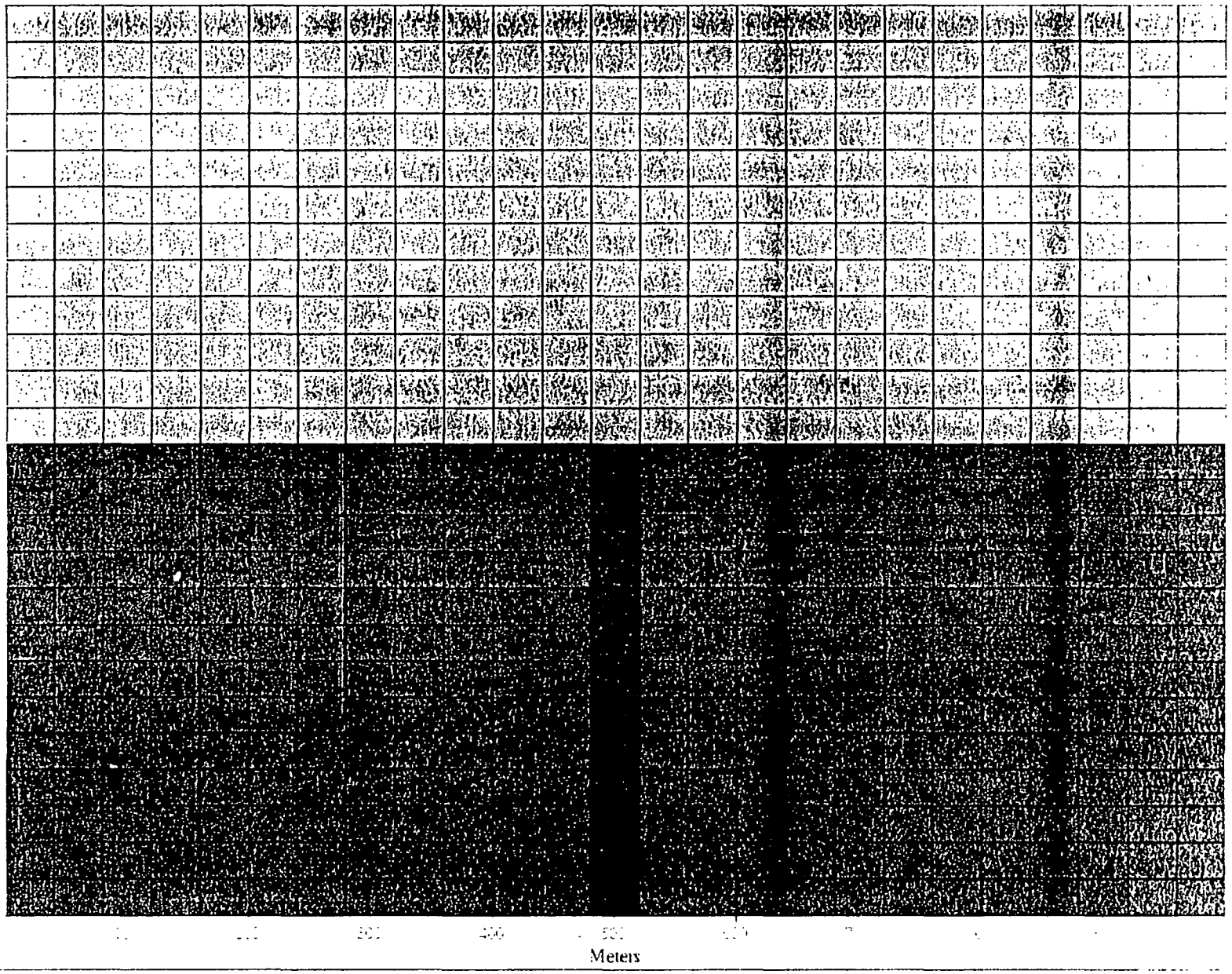

GOVERNING EQUATIONS

Conservation of Fluid Mass:

$$\nabla \cdot (\rho \vec{q}) + \frac{\partial \phi \rho}{\partial t} = 0$$

Conservation of Momentum (Darcy's Law):

$$\vec{q} = -K \mu_r \left[\nabla h + \rho_r \nabla z \right]$$

Conservation of Groundwater Vorticity:

$$\nabla \cdot \left[\frac{K}{|K|} \frac{1}{\rho \mu_r} \nabla \Psi \right] = \frac{\partial \rho_r}{\partial x}$$

Conservation of Thermal Energy:

$$\nabla \cdot (\lambda^* \nabla T) - \rho_f c_f \vec{q} \cdot \nabla T = \left[\phi \rho_f c_f + (1-\phi) \rho_s c_s \right] \frac{\partial T}{\partial t}$$

Conservation of Solute Mass:

$$\nabla \cdot (D \nabla \dot{M}^T_{c,aq}) - \vec{v} \cdot \nabla \dot{M}^T_{c,aq} = \frac{\partial \dot{M}^T_c}{\partial t}$$

Mass Balance:

$$\dot{M}^T_{c,aq} = \phi M_c + \sum_{s=1}^{\hat{s}} \phi \tau_{cs} M_s$$

$$\dot{M}^T_{c,sol} = \sum_{m=1}^{\hat{m}} \tau_{cm} \dot{M}_m$$

$$\dot{M}^T_c = \phi M_c + \sum_{s=1}^{\hat{s}} \phi \tau_{cs} M_s + \sum_{m=1}^{\hat{m}} \tau_{cm} \dot{M}_m$$

Law of Mass Action:

$$K = \prod_i a_i^{\nu_i}$$

TABLE 2 – Summary of the equations governing groundwater flow, heat transport, and reactive solute transport in porous media.

PROGRESS TOWARD A COUPLED HYDROCHEMICAL MODEL

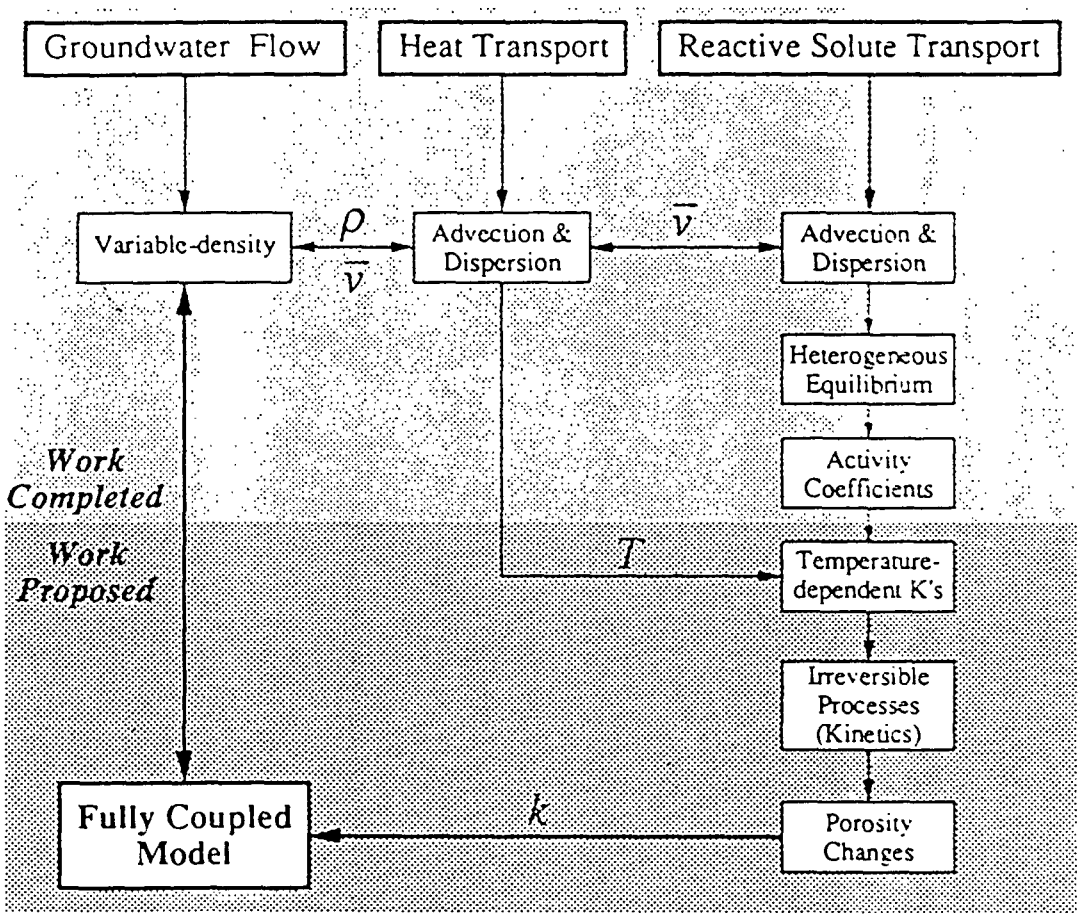

FIGURE 4 – Summary flowchart of progress and proposed coupled modeling efforts.

HYDROCHEMICAL MODELING OF URANIUM DEPOSITS AS ANALOGUES FOR NUCLEAR WASTE REPOSITORIES

NUMERICAL MODEL FEATURES

- 2-D STEADY STATE AND TRANSIENT GROUNDWATER FLOW
- SPATIALL VARIABLE MATERIAL PARAMETERS
- STREAM FUNCTION REPRESENTATION OF FLOW FIELD
- 2-D HEAT TRANSPORT
- VARIABLE-DENSITY FLOW
- 2-D REACTIVE SOLUTE TRANSPORT (LOCAL EQ APPROACH)
- DISPERSION, DIFFUSION
- REDOX REACTIONS
- VARIABLE pH

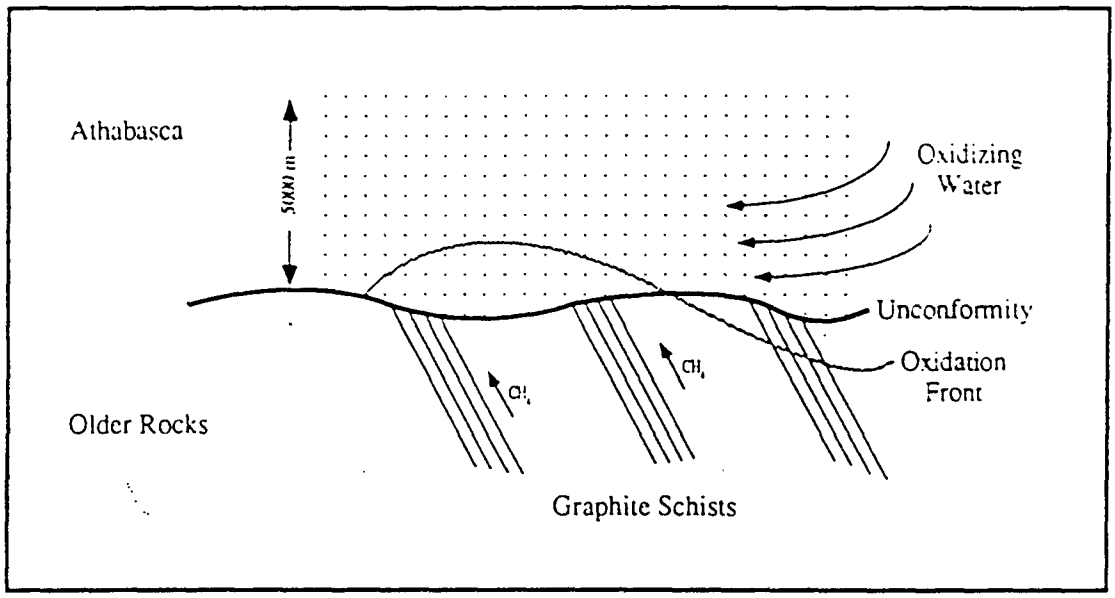

FIGURE 2 – Diagram of the hydrothermal–diagenetic concept for the origin of unconformity–type uranium deposits (after Maynard, 1983).

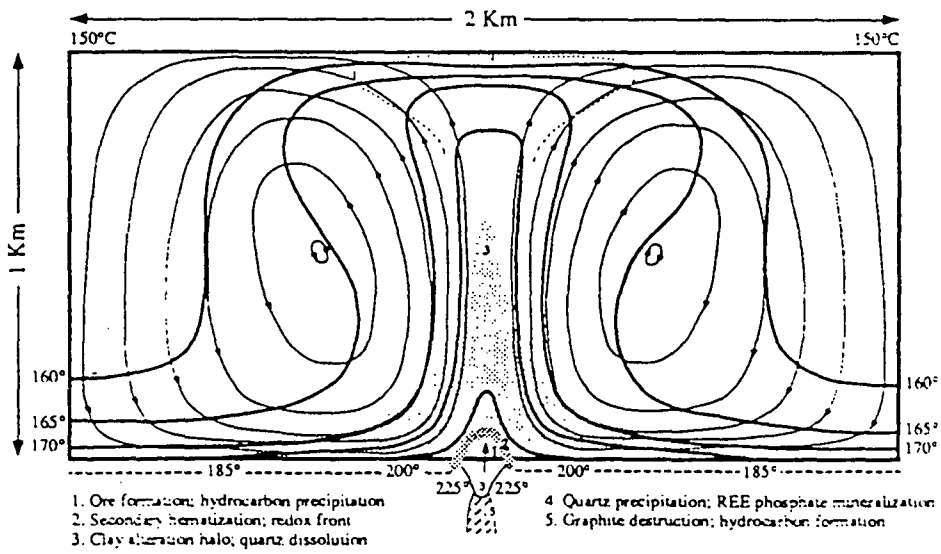

FIGURE 3 – Schematic representation of the hydrothermal–diagenetic convective system as inferred for the formation of unconformity–type uranium deposits in the Athabasca Basin (after Hoeve and Quirt, 1984).

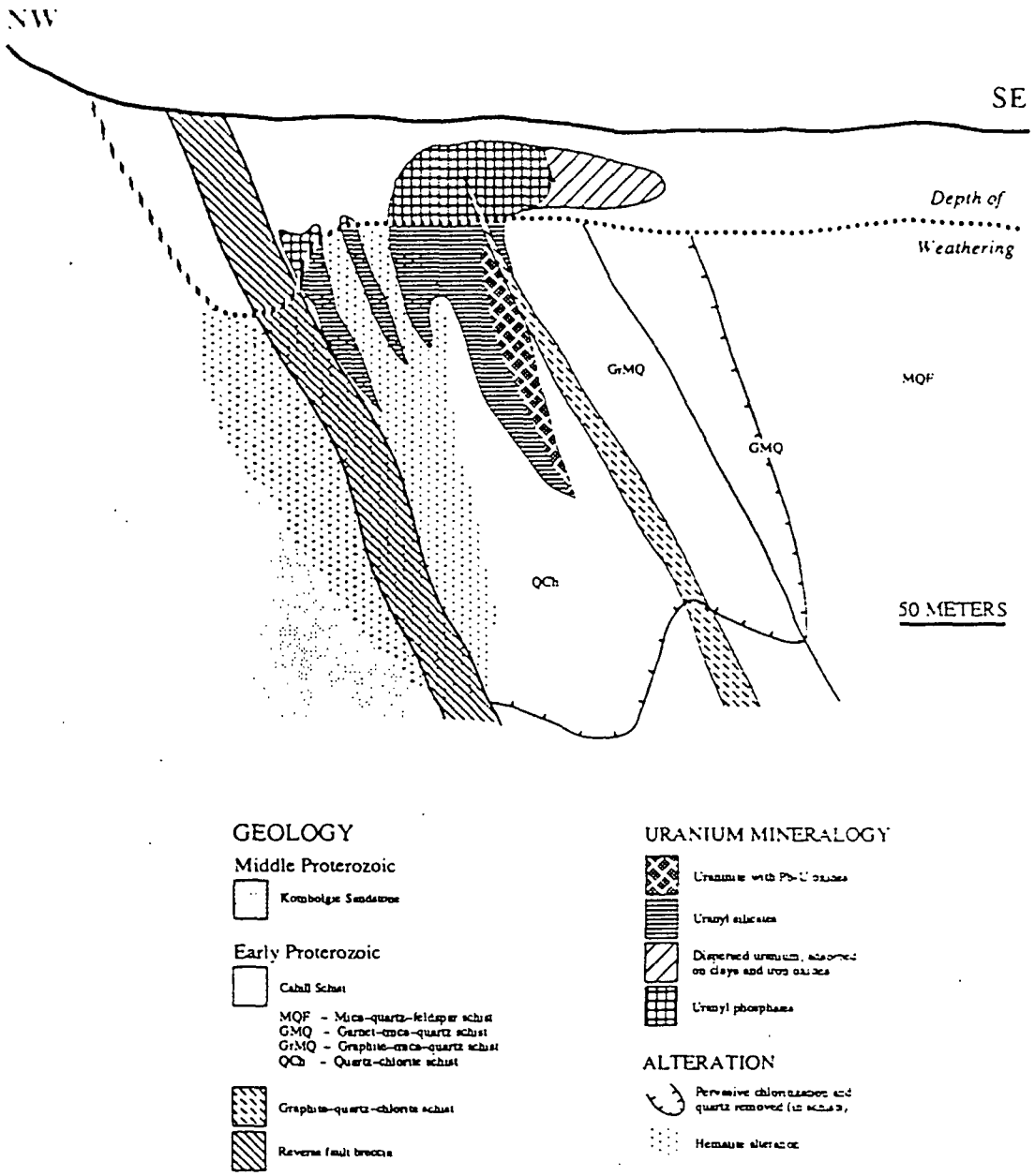

FIGURE 1 – Cross section through the Koongarra uranium deposit (after Snelling, 1989). No vertical exaggeration.

HYDROCHEMICAL MODELING OF URANIUM DEPOSITS AS ANALOGUES FOR NUCLEAR WASTE REPOSITORIES

by
Grant Garven
Associate Professor

Department of Earth and Planetary Sciences
The Johns Hopkins University
Baltimore, Maryland

DOE BRUTON & SHAW (1988) RAN AN EQ6 SIMULATION OF A SPENT FUEL J13 WATER REACTION ASSUMING ATMOSPHERIC PCO2 AND PO2.

HAIWEEITE PRECIPITATED AS THE ONLY URANIUM BEARING MINERAL.

THIS APPEARS TO BE ANALOGOUS TO KOONGARRA. HOWEVER, AS PHOSPHATE ZONE VS. SILICATE ZONE RESULTS SHOW, RESULTS ARE SENSITIVE TO WATER CHEMISTRY AND ASSUMPTIONS ABOUT CONDITIONS.

CONCLUSIONS:

MODEL RESULTS ARE CONSISTENT WITH MODERN FORMATION OF THE URANYL SILICATE ZONE FROM REACTION OF SILICA-RICH WATER WITH URANINITE IN THE VICINITY OF PH 49. SILICA DOES NOT COME FROM THE CHLORITE OR THE QUARTZ IN THE SYSTEM. IT MAY COME FROM FELDSPARS IN THE KOMBOLGIE OR THE CAHILL OUTSIDE OF THE ORE ZONE.

OTHER THAN THE PH 49 WATER AT 28-30 METERS DEPTH U LEVELS ARE TOO LOW AT PRESENT TO FORM URANYL SILICATES. NEARBY URANINITE MAY BE REQUIRED FOR HIGH URANIUM LEVELS IN SOLUTION.

THE URANYL SILICATE DATA BASE PRODUCES THE WRONG MINERALS. CLEARLY THE DATA LACK THE NEEDED PRECISION FOR LICENSING ACTIVITIES.

THE EQ6 MODEL SIMULATED
THE TITRATION REACTION OF
PH 49 SILICATE ZONE WATER
(DELETING MINOR CONSTITUENTS)
WITH URANINITE CHLORITE
AND PYRITE USING KAOLINITE
EQUILIBRIUM TO FIX ALUMINUM
WITH FIXED O2 AND CO2.

MODEL RESULTS WERE:

URANYL SILICATES PRECIPITATED
(HAWEEITE NOT SKLODOWSKITE)
AND A STRONG URANYL CARBONATE
SOLUTION EVOLVED WITH REACTION
PROGRESS. CONTINUED DISSOLUTION
OF CO2 PRODUCED ULTIMATE
DISSOLUTION OF ALL URANIUM.
GIBBSITE, SAPONITE, HEMATITE,
CALCIUM/MAGNESIUM CARBONATE
AND PYROLUSITE ALSO FORMED.
SILICA ACTIVITIES DROPPED BELOW
QUARTZ SATURATION LEVELS.

EQ6 MODELLING OF PH 49 TITRATION WITH URANINITE

STARTS WITH URANYL SILICATES

EVOLVES TO $UO_{2.25}$ SOLID AT MEASURED EH

CONCLUSION

A MORE OXIDIZING WATER THAN MODELLED USING THE MEASURED EH IS NEEDED TO PRODUCE URANYL SILICATES OR THE MODEL OF O_2 AND SILICA INPUT IS TOO SIMPLE.

TABLE IV. EQ3 MODELLING OF PH55 MAJOR GROUNDWATER SPECIES AND SATURATED SOLIDS

SPECIES	LOG ACTIVITY
HCO3-	-2.79
CO2(AQ)	-3.05
MG++	-3.21
SIO2(AQ)	-3.29
CL-	-3.83
CA++	-4.28
NA+	-4.24
FE++	-4.37

MINERAL	LOG Q/K
CHALCEDONY	0.440
COPPER	-0.013
CRISTOBALITE	-0.161
GOETHITE	3.154
HEMATITE	7.268
KAOLINITE	0.928
MAGNETITE	5.736
QUARTZ	0.711
SMECTITE CLAYS SATD.	
THORIANITE	4.451
WITHERITE	-0.078

TABLE III. EQ3 MODELLING OF PH 49 MAJOR GROUNDWATER SPECIES AND SATURATED SOLIDS

SPECIES	LOG ACTIVITY
HCO3-	-2.70
MG++	-3.10
CO2(AQ)	-3.19
SIO2(AQ)	-3.49
CL-	-3.65
CA++	-4.01
NA+	-4.31

MINERAL	LOG Q/K
CHALCEDONY	0.243
CRISTOBALITE	-0.037
GOETHITE	4.720
HAIWEEITE	0.802
HEMATITE	9.501
MAGNETITE	7.916
QUARTZ	0.514
SODDYITE	1.123
THORIANITE	4.518
WITHERITE	-0.077

TABLE II. Concentrations (in ug g-1 unless indicated) in the water collected in Nov. 1988 (from Bockting and Wijland in Duerden (13)).

Well	Depth (m)	Al	B	Ba	Ca	K	Mg	Mn	Na	Si
PH49	28-30	<0.01	0.014	0.011	5.2	0.75	25	0.140	1.2	9.2
PH55	40-42	<0.01	0.009	0.023	2.7	1.10	19	0.096	1.4	14.5
PH58	38-40	<0.01	0.008	0.049	2.1	1.30	18	0.075	2.2	15.7
PH94	40-42	<0.01	0.009	0.003	0.7	1.00	6	0.006	2.1	12.1
KD1	40-42	<0.01	0.006	0.005	2.3	0.41	5	0.120	1.0	5.3

Well	Depth (m)	Fe	V	As	Se (mg/l)	Pb	Th	Ti	Zn	Cu
PH49	28-30	1.1	0.97	0.72	1.46	1.05	0.07	<0.002	0.006	2.3
PH55	40-42	3.5	0.60	0.35	<0.7	0.69	0.06	<0.002	<0.002	.
PH58	38-40	1.1	1.41	1.21	3.98	0.68	0.06	<0.002	0.004	2.4
PH94	40-42	0.1	2.19	0.29	<1.1	1.07	0.10	<0.002	<0.002	1.6
KD1	40-42	22.0	0.62	0.92	2.26	0.98	0.09	<0.002	<0.002	3.2

Well	Depth (m)	TOC	HCO3	D.O.	Eh (mV)	pH	U	PO4 (ug/l)	Cl	F	SO4
PH49	28-30	1.51	159	230	130	6.84	93.9	0.090	8.5	0.34	0.29
PH55	40-42	1.38	120	198	75	6.60	0.98	0.445	5.5	0.24	0.24
PH58	38-40	1.24	114	187	135	6.59	1.05	0.665	6.2	0.21	0.10
PH94	40-42	1.58	38	90	225	6.94	0.28	0.200	3.4	0.11	0.84
KD1	40-42	1.42	81	126	140	6.07	0.52	0.010	3.1	0.12	<0.02

TABLE I. List of secondary uranium minerals.
* denotes that the minerals are included in the EQ3/6 database.

Secondary uranium minerals at Koongarra, from Snelling (5)

Oxides	
Curite	$2(PbO)5(UO_3).5H_2O$
Fourmanite	$(PbO)4(UO_3).4H_2O$
Vandendriesschite	$(PbO)7(UO_3).12H_2O$
Silicates	
* Kasolite	$Pb(UO_2)(SiO_2).H_2O$
* Sklodowskite	$Mg(UO_2)_2(Si_2O_7).6H_2O$
* Uranophane	$Ca(UO_2)_2(Si_2O_7).6H_2O$
Phosphates	
* Saleeite	$Mg(UO_2)_2(PO_4)_2.8-10H_2O$
Sabulgalite	$HAl(UO_2)_4(PO_4)_2.16H_2O$
Metatorbernite	$Cu(UO_2)_2(PO_4)_2.8H_2O$
* Torbernite	$Cu(UO_2)_2(PO_4)_2.8-12H_2O$
Renardite	$Pb(UO_2)_4(PO_4)_2(OH)_4.7H_2O$
Dewindtite	$Pb(UO_2)_2(PO_4)_2.3H_2O$
Sulfates	
Johannite	$Cu(UO_2)_2(SO_4)_2.6H_2O$
Vanadates	
* Carnotite	$K_2(UO_2)_2(VO_4)_2.3H_2O$
* Tyuyamunite	$Ca(UO_2)_2(VO_4)_2.5-8H_2O$

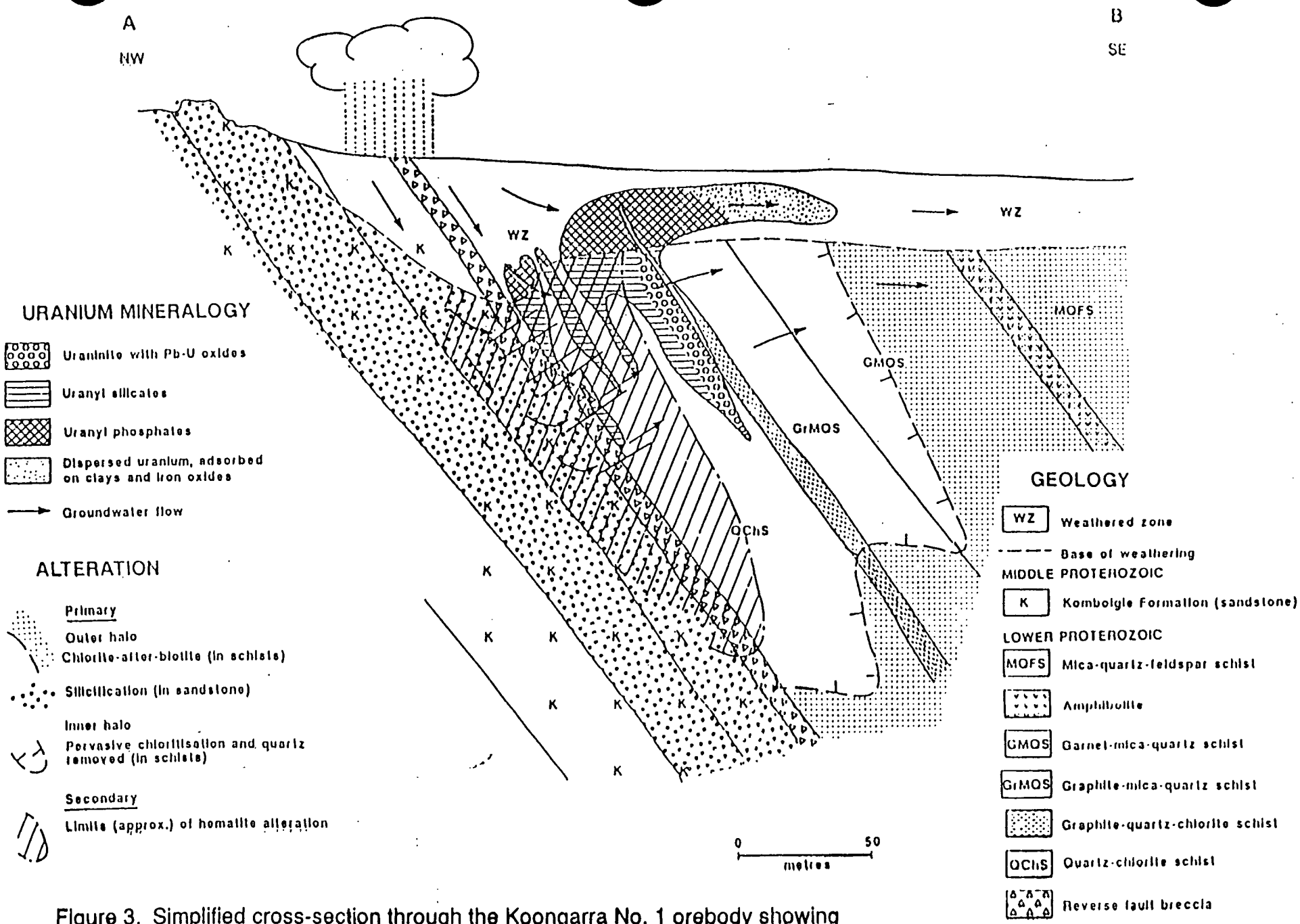

Figure 3. Simplified cross-section through the Koongarra No. 1 orebody showing geology, distribution of uranium minerals, distribution of alteration, and present groundwater flow.

Figure 1. Regional geology map showing the location of the Koongarra uranium deposit.

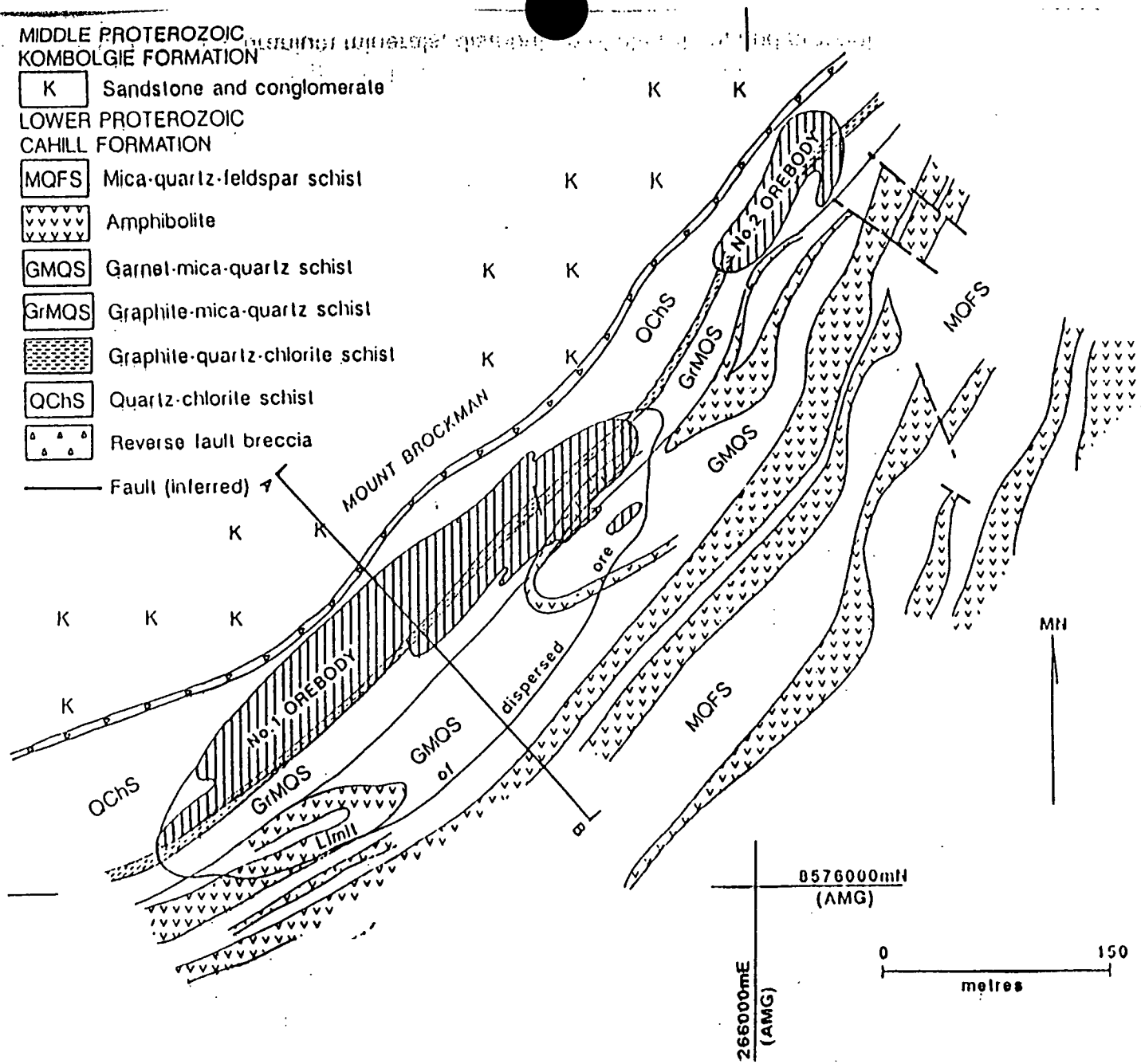

Figure 2. Local geology map showing the location of the Koongarra No. 1 and No. 2 orebodies. Because of surficial cover the geological units and outline of the mineralisation are projected to the surface from the base of weathering.

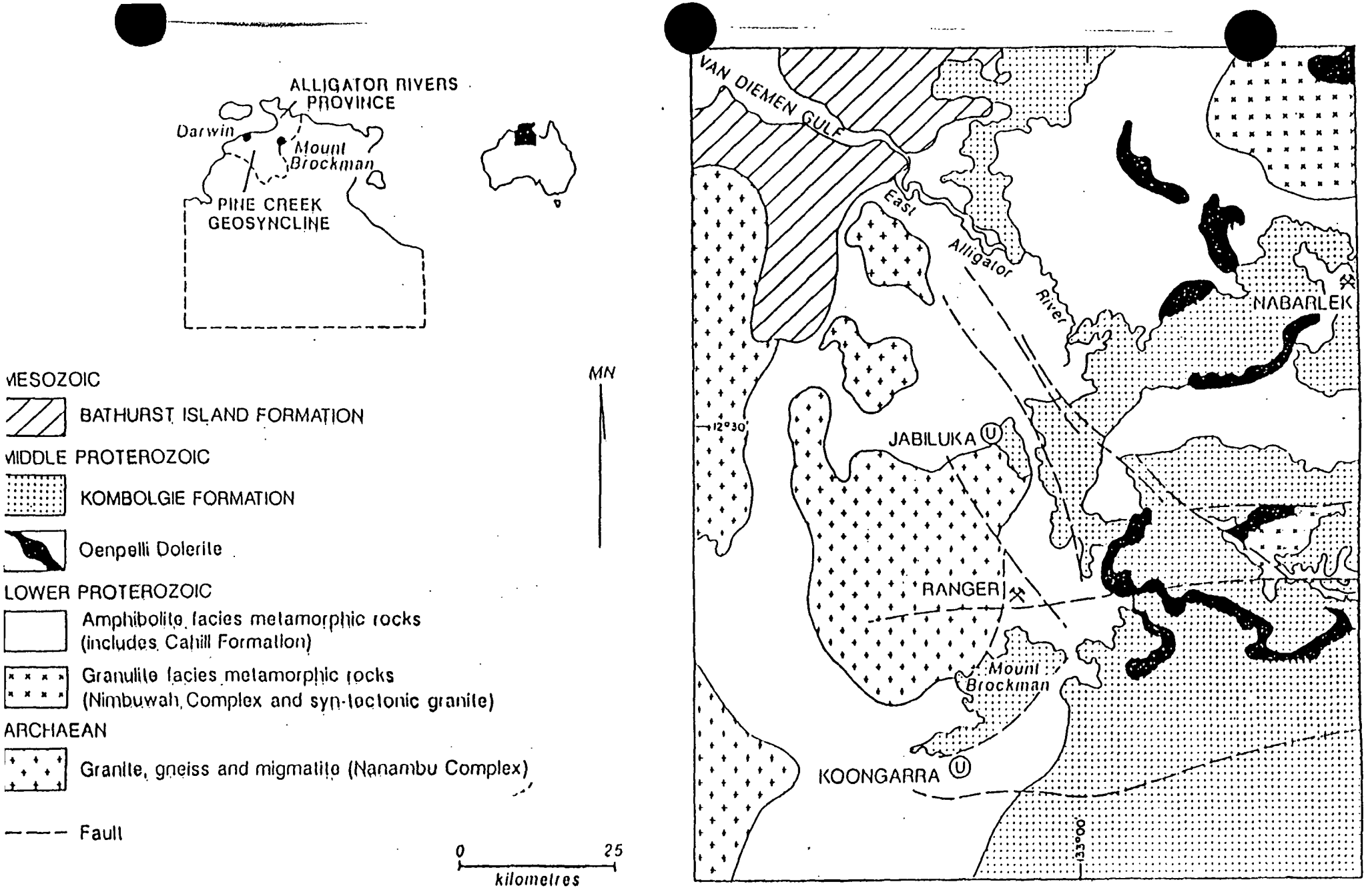

Figure 1. Regional geology map showing the location of the Koongarra uranium deposit.

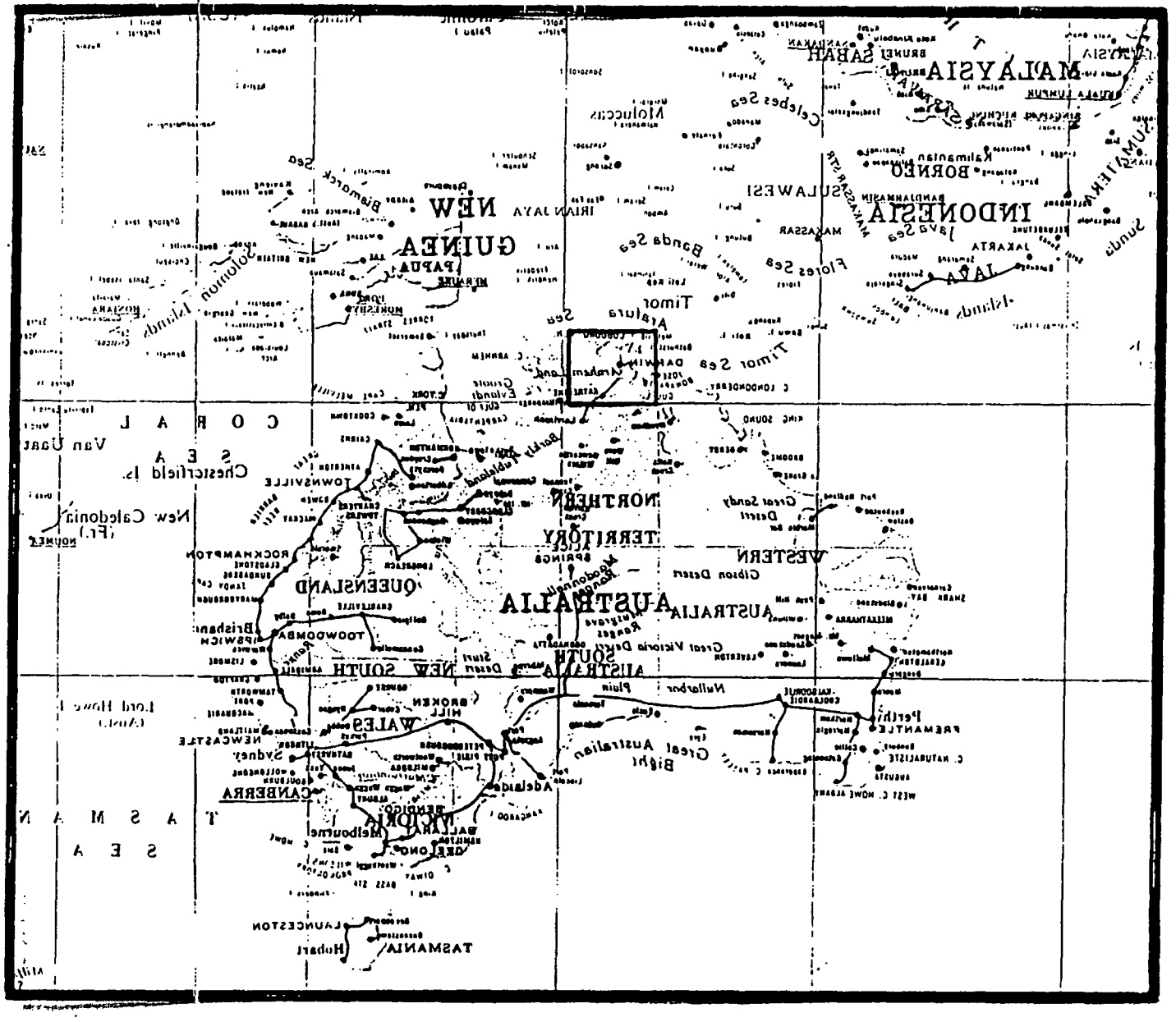
TASMANIA
Hobart
LAUNCESTON
VICTORIA
Melbourne
CANBERRA
Sydney
NEW SOUTH WALES
Adelaide
SOUTH AUSTRALIA
Great Australian Bight
Perth
FREMANTLE
WESTERN AUSTRALIA
NORTHERN TERRITORY
QUEENSLAND
Brisbane
TOWNSVILLE
CAIRNS
NEW GUINEA
PAPUA
Timor Sea
Arafura Sea
Banda Sea
Flores Sea
Celebes Sea
Molucca Sea
INDONESIA
JAVA
JAKARTA
SULAWESI
BORNEO
MALAYSIA
SABAH
BRUNEI
Solomon Islands
Bismarck Sea
Coral Sea
Tasman Sea
New Caledonia (Fr.)
Lord Howe Island

FIGURE 1

VALLES CALDERA NATURAL ANALOGUE STUDY RESULTS

- LITTLE EVIDENCE OF MIGRATION AS CONSEQUENCE OF THERMAL ENVIRONMENT
- STEAM LEACHING OF FLUORINE AND CHLORINE FROM TUFF
- TRANSPORT OF HALOGENS IN VAPOR PHASE
- FLUID AND VAPOR FLOW APPEARS TO BE IN CHANNELS CONTROLLED BY LOCAL PERMEABILITY

CONCLUSIONS

1) There is no evidence, from bulk chemistry, for transport of non-volatile elements in response to the heating event.

2) The tuff near the obsidian-tuff contact was partly devitrified and depleted in Cl, apparently as a result of heating by the obsidian flow.

3) Cl and F show divergent behavior below the contact, possibly due to the deposition of a F-rich phase, or biotite and amphibole control on F. Experiments predict divergence in the behavior of F and Cl, but there is no simple way to use the experimental results to interpret the site 13 trends.

4) There are few systematic changes in mineralogy with distance from the contact. Cristobalite is more abundant near the contact, which may simply reflect the greater devitrification of these samples; however, textural evidence hints that at least part of the cristobalite is a coating, rather than a a simple devitrification product.

5) Absolute chronology of the various units is still uncertain, but there is evidence that the Banco Bonito is actually two units, separated by 0.2 Ma.

REFERENCES

Daniels, W.R., K. Wolfsberg, R.S. Rundberg and others (1982) **Summary Report on the Geochemistry of Yucca Mountain and Environs.** J. Heiken (ed.), LA-9328-MS, Los Alamos National Laboratory, Los Alamos, NM.

Lambert, S.J. and S. Epstein (1980) Stable isotope investigations of an active geothermal system in Valles Caldera, Jemez Mountains, New Mexico. **Jour Volcanology and Geothermal Res 8,** 111-129.

Self, S., D.E. Kircher and J.A. Wolff (1988) The El Cajete Series, Valles Caldera, New Mexico. **Jour Geophysical Res 93 no. B6,** 6113—6127.

Self, S., J.A. Wolff and T.L. Spell (1990) Stratigraphic and volcanological significance of the volcanic section of the CSDP VC-1 core hole, Valles Caldera, New Mexico. **Trans American Geophysical Union 71 no.43,** 1693.

Spell, T.L. and P.R. Kyle (1989) Petrogenesis of the Valle Grande member rhyolites, Valles Caldera, New Mexico: implications for evolution of the Jemez Mountains magmatic system. **Jour Geophysical Res 94 no. B8,** 10379-10396.

Westrich, H.R., H.W. Stockman and J.C. Eichelberger (1988) Degassing of rhyolitic magma during ascent and emplacement. **Jour Geophysical Res 93 no. B6,** 6503—6511.

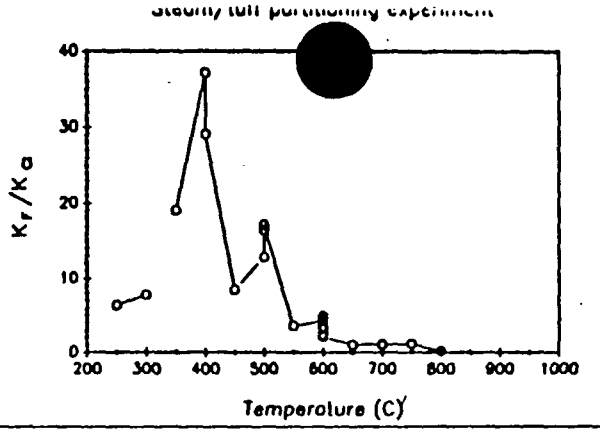
Steam/tuff partitioning experiment
K_r/K_a
Temperature (C)

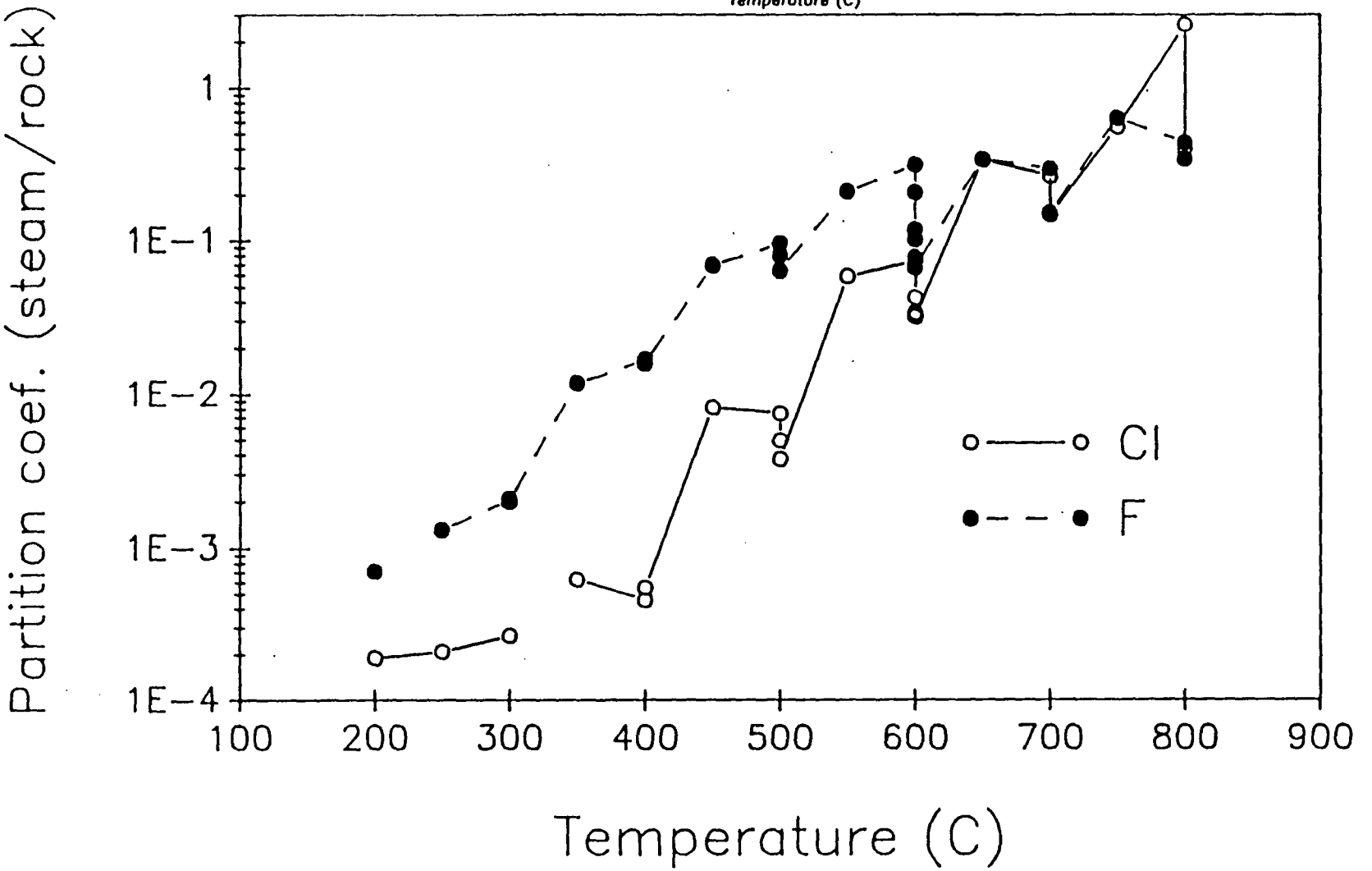
Partition coef. (steam/rock)
1
1E−1
1E−2
1E−3
1E−4
100
200
300
400
500
600
700
800
900
Temperature (C)
Cl
F

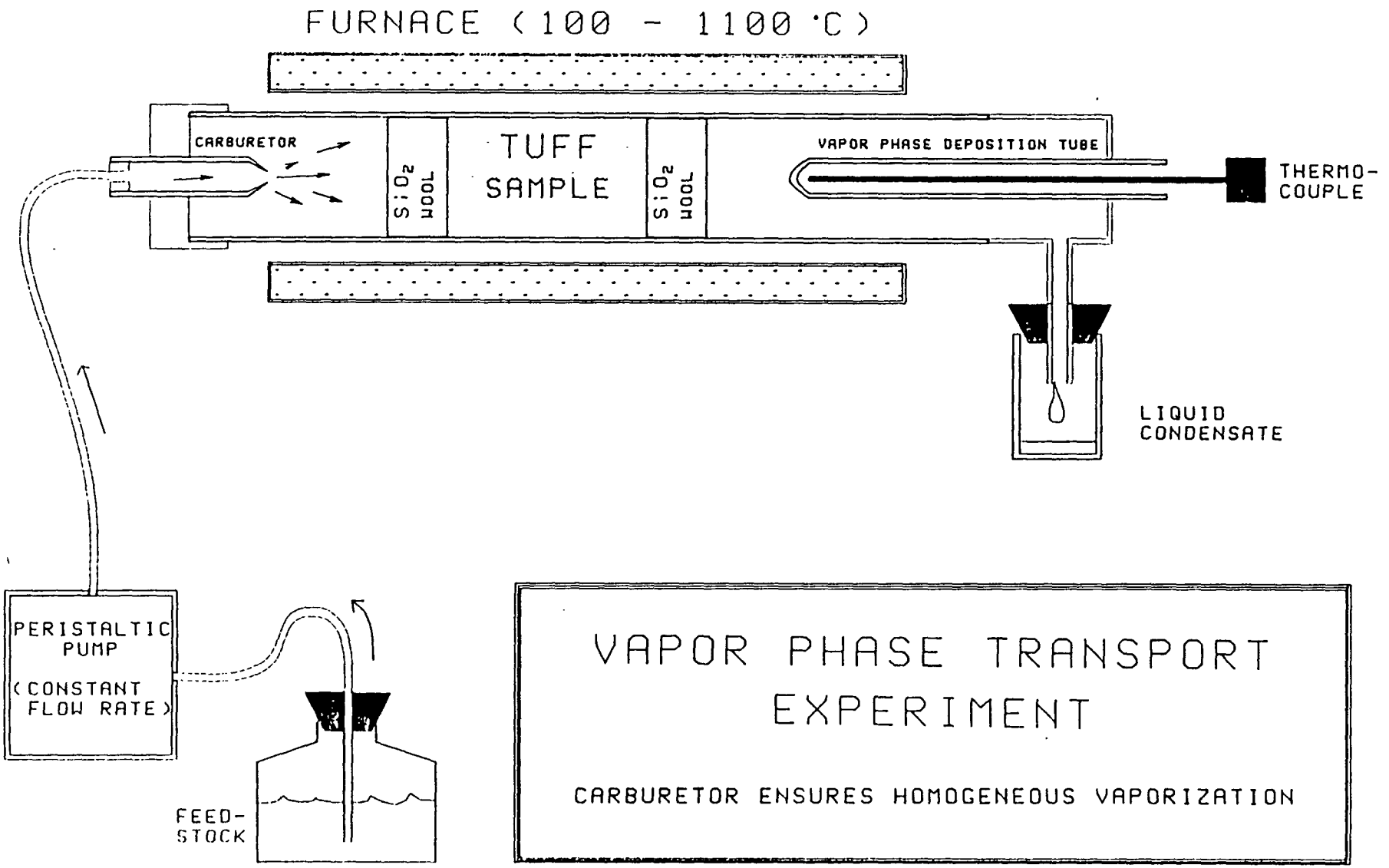

VAPOR PHASE TRANSPORT EXPERIMENT

CARBURETOR ENSURES HOMOGENEOUS VAPORIZATION

VALLES CALDERA NATURAL ANALOGUE STUDY
EXPERIMENTAL STUDY

OBJECTIVE:

TO MODEL BEHAVIOR OF F, Cl AND MOBILE METALS DURING THE HEATING OF THE TUFF.

NATURAL CONDITIONS:

UNSATURATED, STEAM/TUFF ENVIRONMENT DURING THERMAL EVENT

EXPERIMENTAL CONDITIONS:

STEAM/TUFF PARTITION COEFFICIENTS $f(T)$ $125<T<800$

STEAM ENVIRONMENT, RELEASE OF F, Cl AND Na
$f(t)$ T=CONSTANT

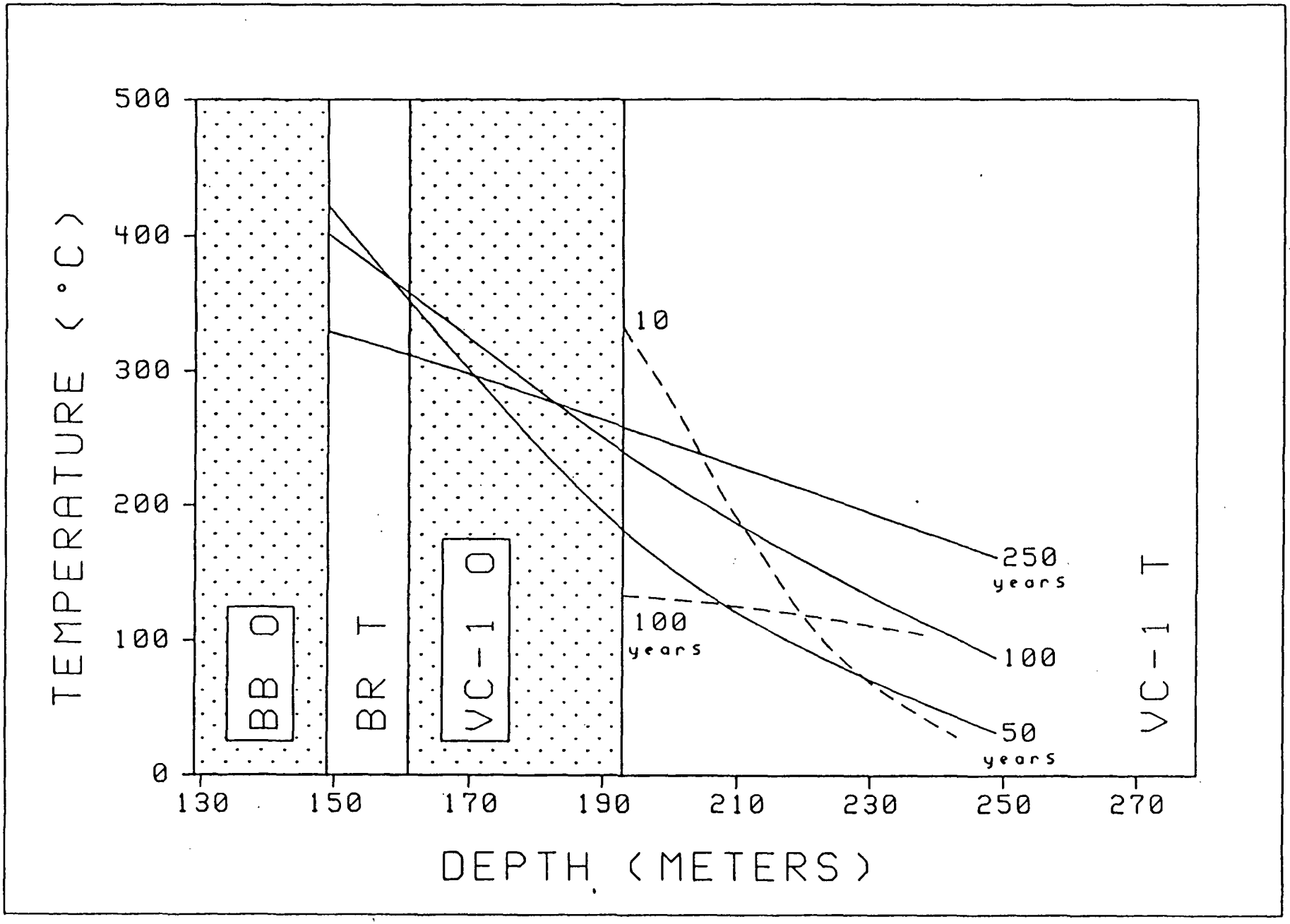
TEMPERATURE (°C)
500
400
300
200
100
0
130
150
170
190
210
230
250
270
DEPTH (METERS)
BB O
BR T
VC-1 O
VC-1 T
10
100 years
250 years
100
50 years

The divergent behavior of F and Cl is consistent with previous studies of devitrification at Obsidian Dome in the Inyo Chain of California (Westrich et al., 1988), where it was found that the F/Cl tended to increase during devitrification.

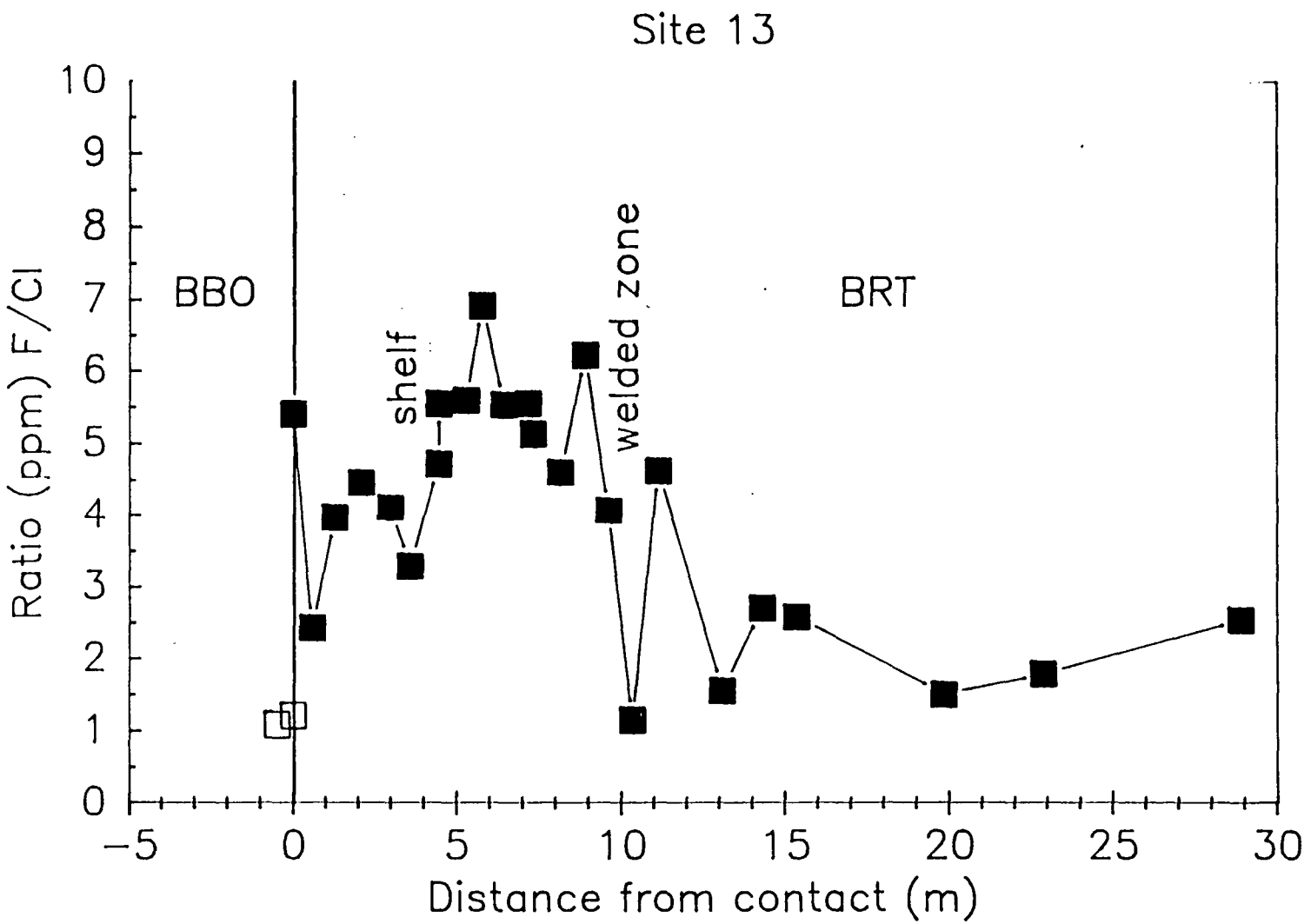

On a Ba/Ta vs. Th/Ta plot, the site 13 tuff samples (open circles) appear to continue the Valles evolution trend found by Spell and Kyle (1989). Samples of tuff and obsidian near the BBO-BRT contact, collected from the VC-1 corehole (X's), overlap the site 13 data but show more scatter. Overall, we find few systematic differences between the compositions of the upper BRT and the lower BBO.

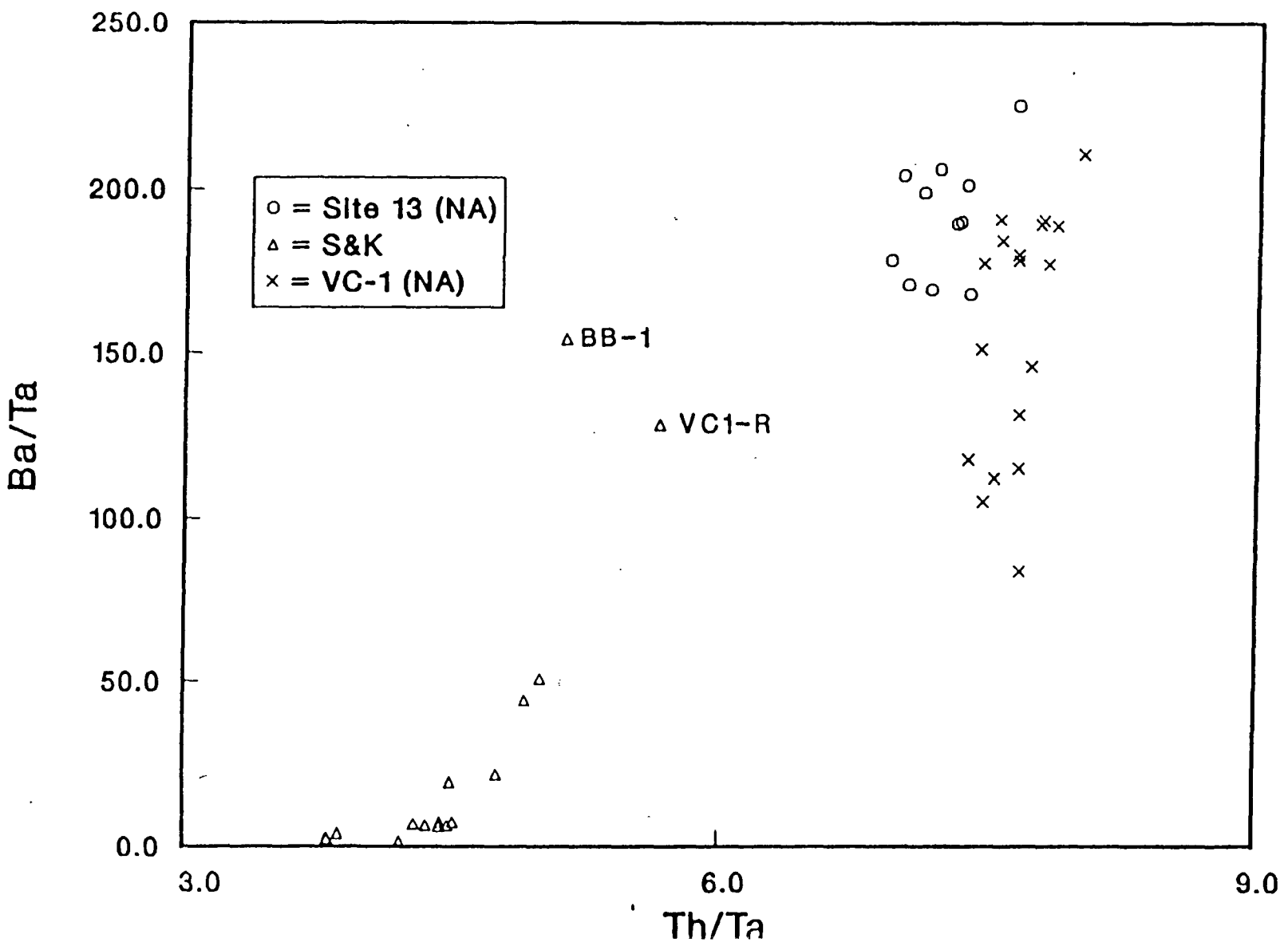

which is upper BRT lower BBO

$^{40}Ar/^{39}Ar$ Dates

Sample	Location	Date (Ma)	Mineral
Upper Banco Bonito Obsidian	corehole	0.235 ±0.037	glass
Lower Banco Bonito Obsidian	outcrop	0.451 ±0.023 0.439 ±0.020 0.515 ±0.112	biotite glass plagioclase
Battleship Rock Tuff	outcrop	0.410 ±0.056 0.280 ±0.054	sanidine biotite
Battleship Rock Tuff	outcrop	0.555 ±0.021	sanidine
Battleship Rock Tuff	outcrop	0.464 ±0.056 0.241 ±0.043	biotite plagioclase
VC-1 Obsidian	corehole	0.861 ±0.144 0.800 ±0.055	glass glass

The absolute ages of the BBO and BRT are not well known. Self *et al.* (1988) originally suggested that the BRT, the BBO, and the intervening El Cajete pumice were all erupted over a short period (as little as 50 years) ≈ 0.150±0.020 Ma b.p. More recently, Self *et al.* (1990) obtained an age of 0.195±0.035 Ma for the upper BBO, and 0.330±0.030 Ma for the El Cajete pumice, suggesting that the BRT is at least 0.330 Ma old. The latter results seem more consistent with the fact that deep canyons were incised in the BRT at the time of eruption of the BBO. In an attempt to clarify the chronology, we submitted samples of fresh site 13 glass, feldspar, and biotite for step-wise $^{39}Ar/^{40}Ar$ age determinations, for both the BBO and the BRT. In addition, we submitted samples of upper BBO and a stratigraphically lower obsidian (the so-called "VC-1 obsidian") from the VC-1 drill hole, and a sample of 600 year-old Obsidian Dome glass as a control. Results of our $^{39}Ar/^{40}Ar$ determinations are summarized above. Within error, our age for the upper BBO agrees with the results of Self *et al.* (1990), and our age for the BRT is consistent with their results for El Cajete pumice. At site 13, we are unable to distinguish the between the ages of the BBO and BRT, but the error in the determinations is so large that several tens of thousands of years could have separated the emplacement of the two units. It is possible that the upper BBO sampled in the corehole, and the lower BBO sampled at site 13 were emplaced at very different times.

Non-volatile trace elements show little variation with distance from the contact. Co is erratic and tracks Fe concentration, since both elements are controlled by the minor (≈ 1%) amounts of Fe oxides, micas, amphiboles and pyroxenes in the samples. There is no obvious correlation of bulk Fe and Co with the pinkness (hence secondary hematite content) of the tuff. Cs is slightly higher near the contact; we have observed this trend at two other BBO-BRT sites. However, Cs roughly tracks K, and the variations in alkali content may simply reflect variations in the preheating composition of the tuffs.

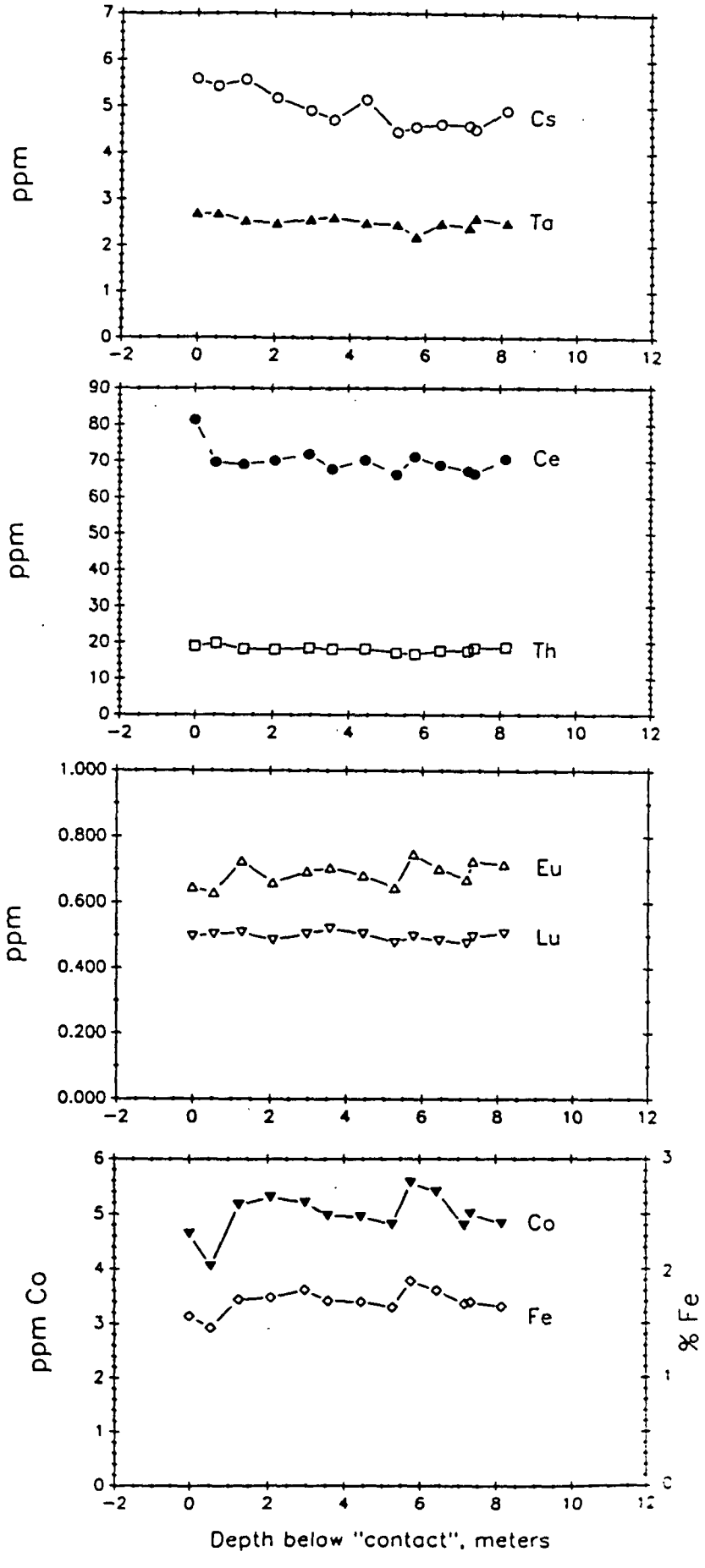

Major element compositions of the tuffs show little variation with distance from the contact. Models for alteration of tuffs in the vicinity of a waste repository (Daniels et al., 1982) suggest SiO_2 will be mobilized; we see no evidence for this mobility in bulk analyses (though there is some microscopic evidence). The weak covariation of F and Fe suggests some amphibole or mica control of F contents, though the amounts of these phases is very small (≈ 1%).

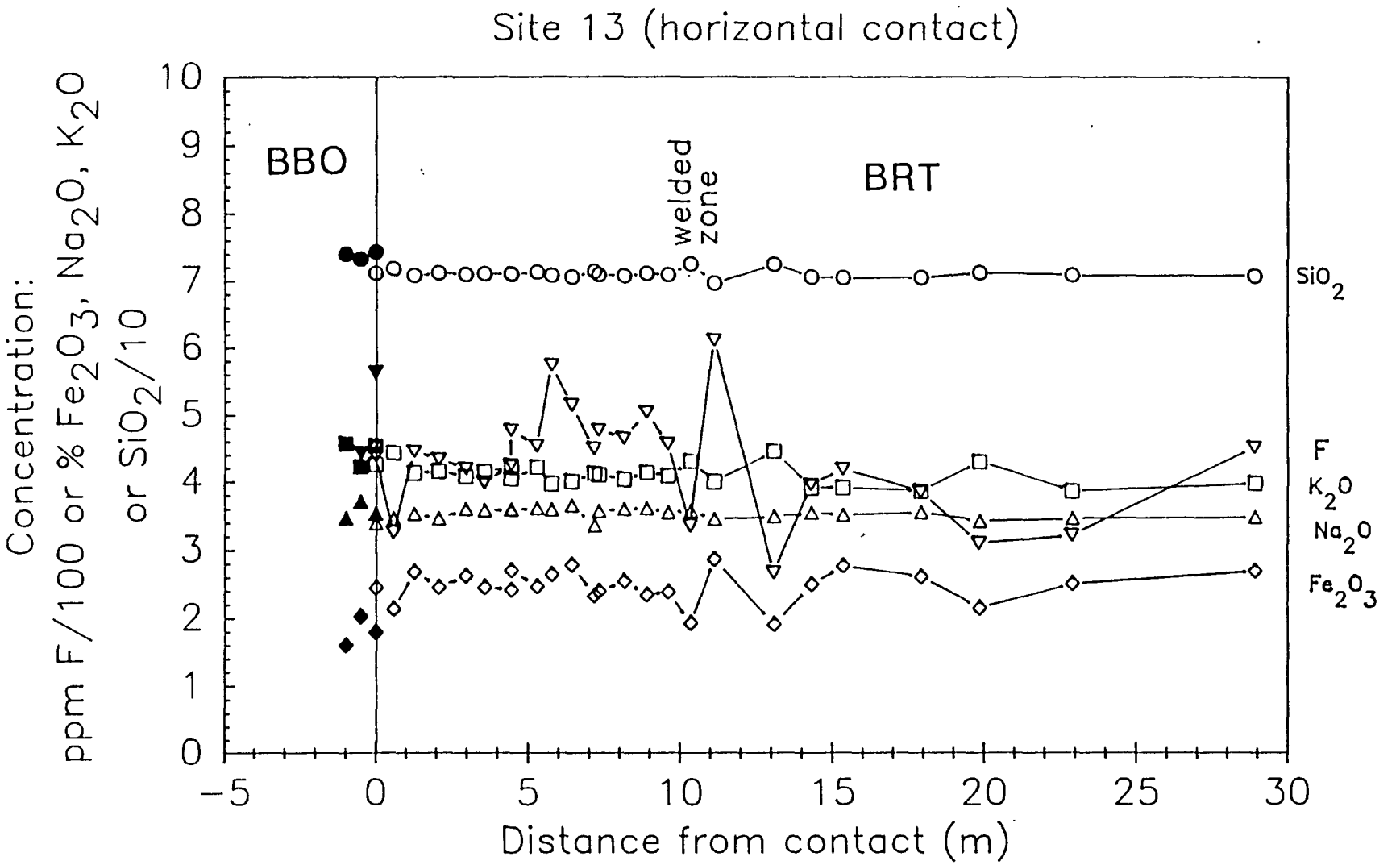

Parti devitrification and loss of Cl and H_2O e occurred in the tuffs closest to the contact. Som dels for radionuclide transport near waste repositories assume Cl can be treated as a conservative tracer; this assumption appears to be invalid at site 13. The D/H shows no systematic variation; the site 13 average of -101±7 °/∞ is close to the average values for meteoric water (-90 °/∞) and devitrified tuff (-125 °/∞, 1.32% H_2O) from the Valles Caldera (Lambert and Epstein, 1979).

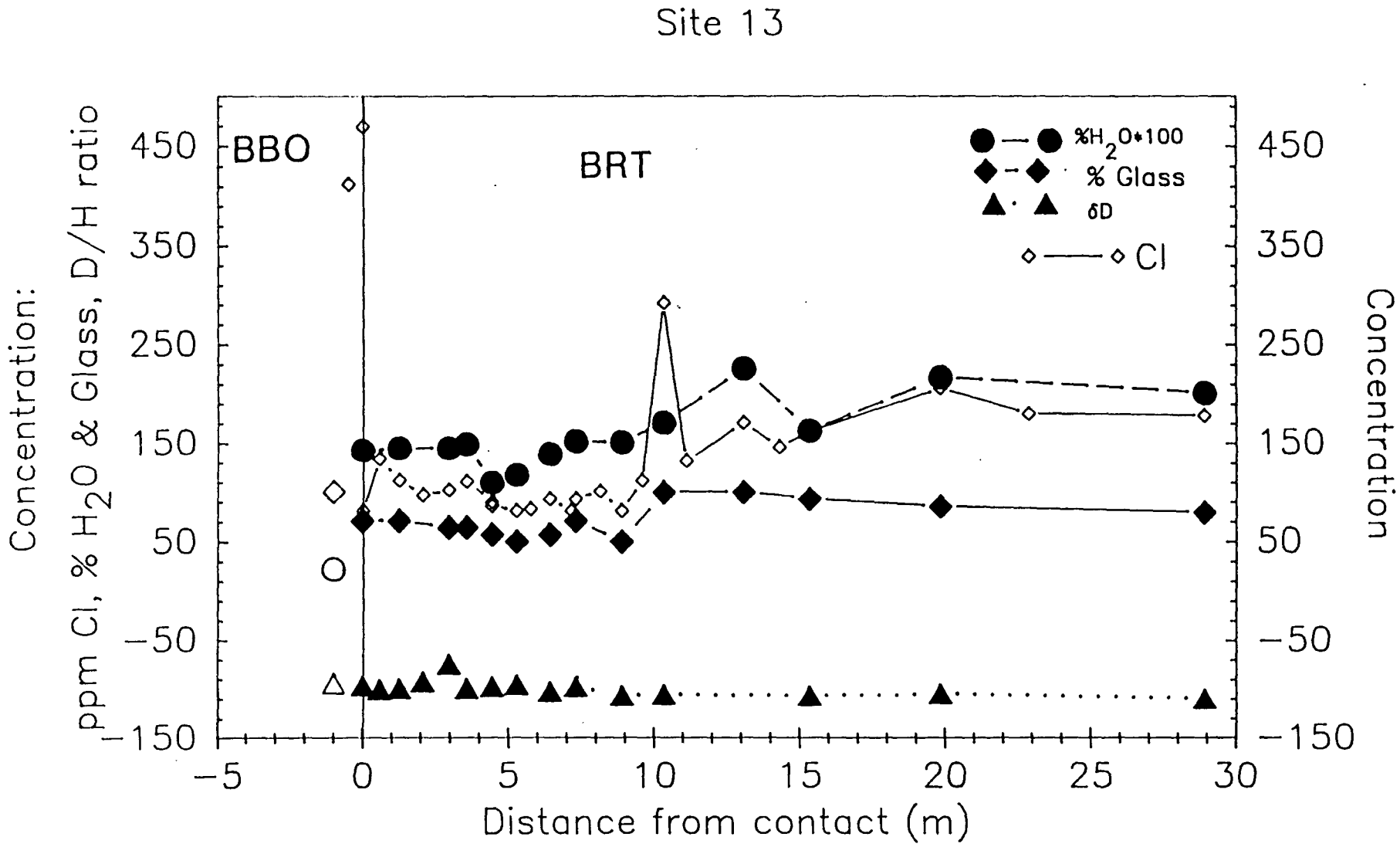

X-Ray Patterns of Tuff Samples from Above (A) and Below (B) the Welded Zone, Site 13

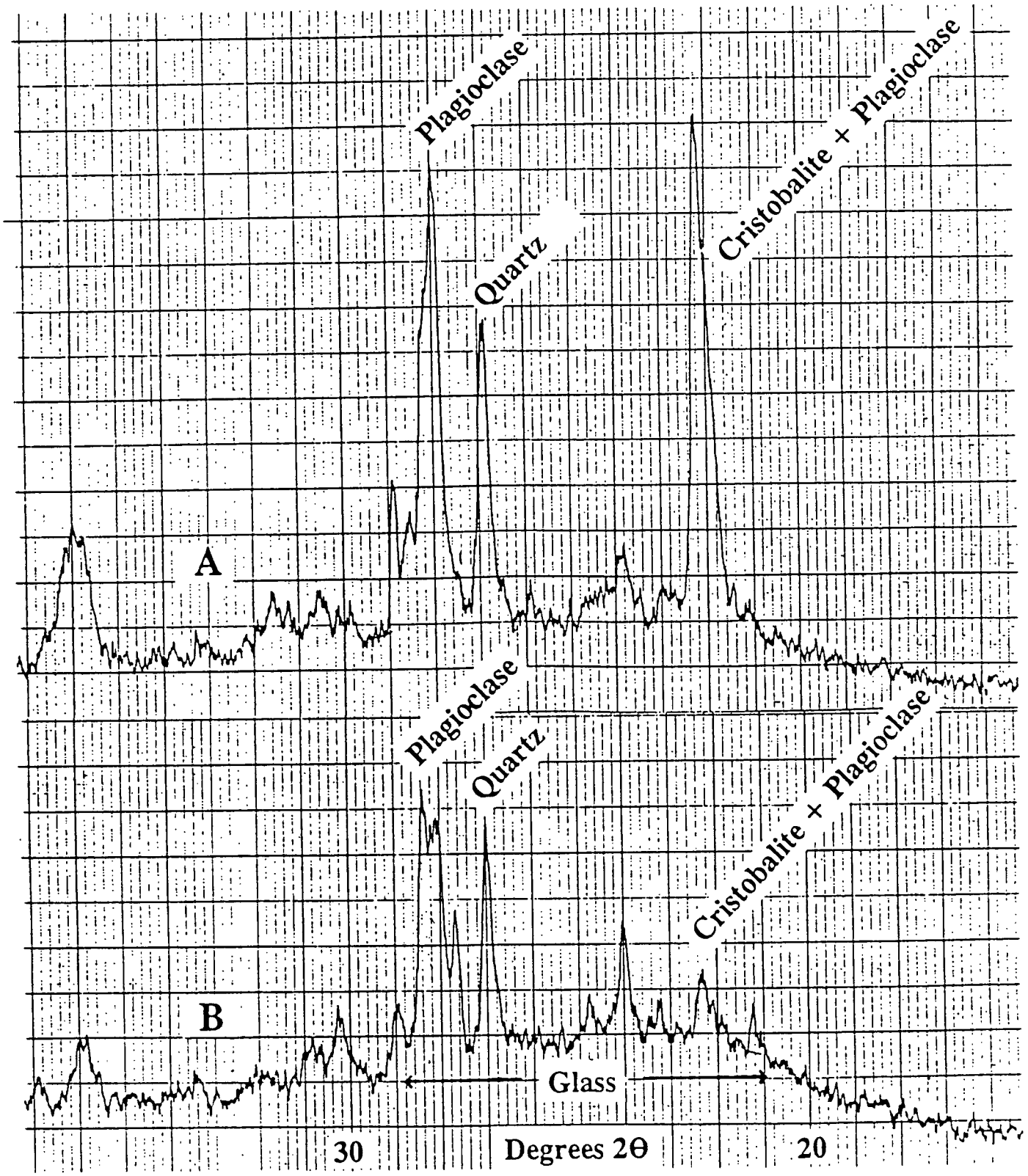

VALLES CALDERA NATURAL ANALOGUE STUDY
INVESTIGATIONS

- FIELD INVESTIGATIONS
  Mapping, sample collection
- LABORATORY INVESTIGATIONS
  Mineralogy
  Texture
  Major, minor, and rare-earth elements
  Glass content
  Volatiles
  $\delta D/H$
  Hydrothermal Steam Flow-through experiments
- MODELLING
  Thermal
  Chemical

Schematic cross-section near VC-1 corehole

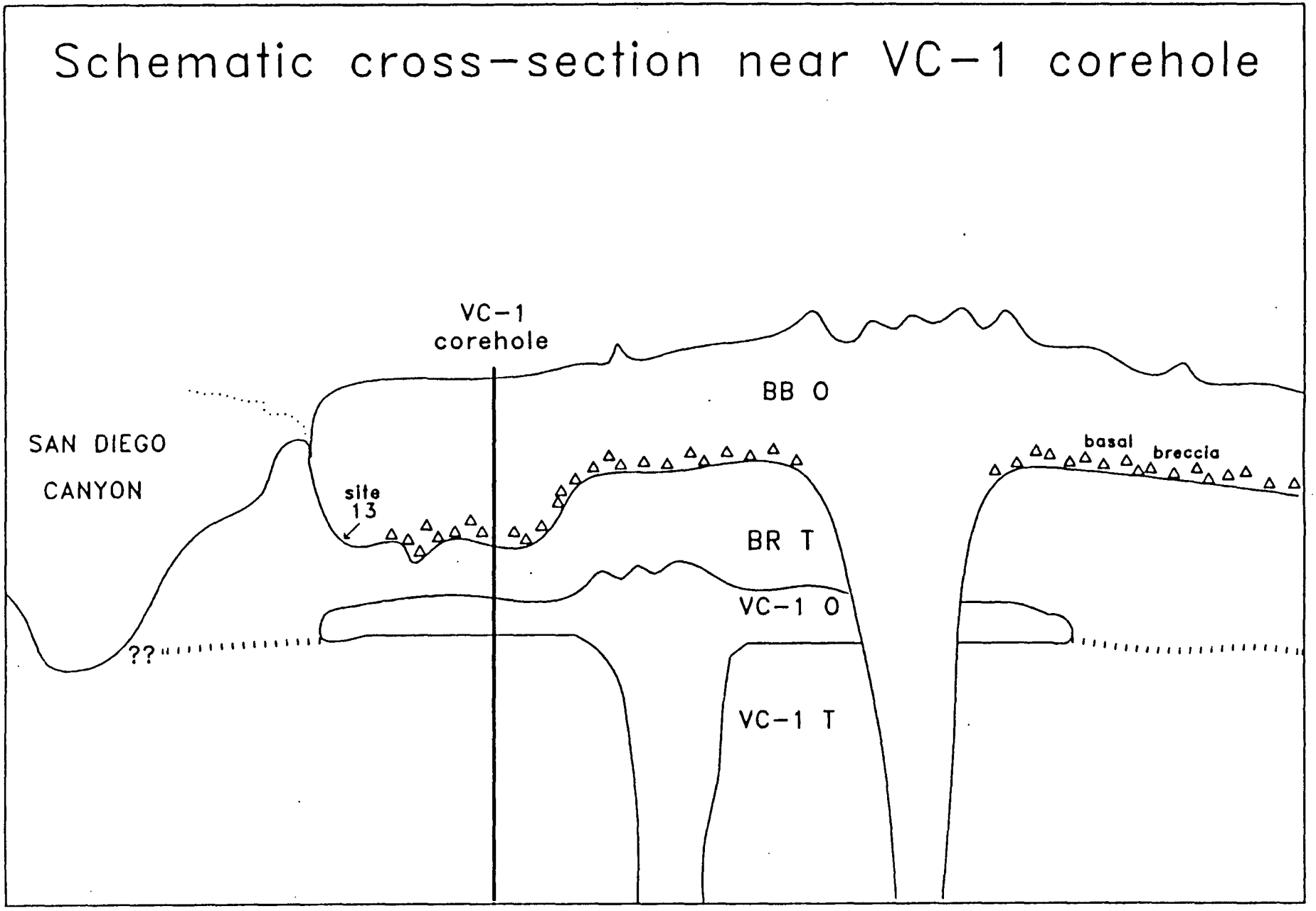

BB O = Banco Bonito Obsidian Flow BR T = Battleship Rock Tuff

VC-1 O = VC-1 Obsidian Flow VC-1 T = VC-1 Tuff

LOCATIONS OF SITES STUDIED

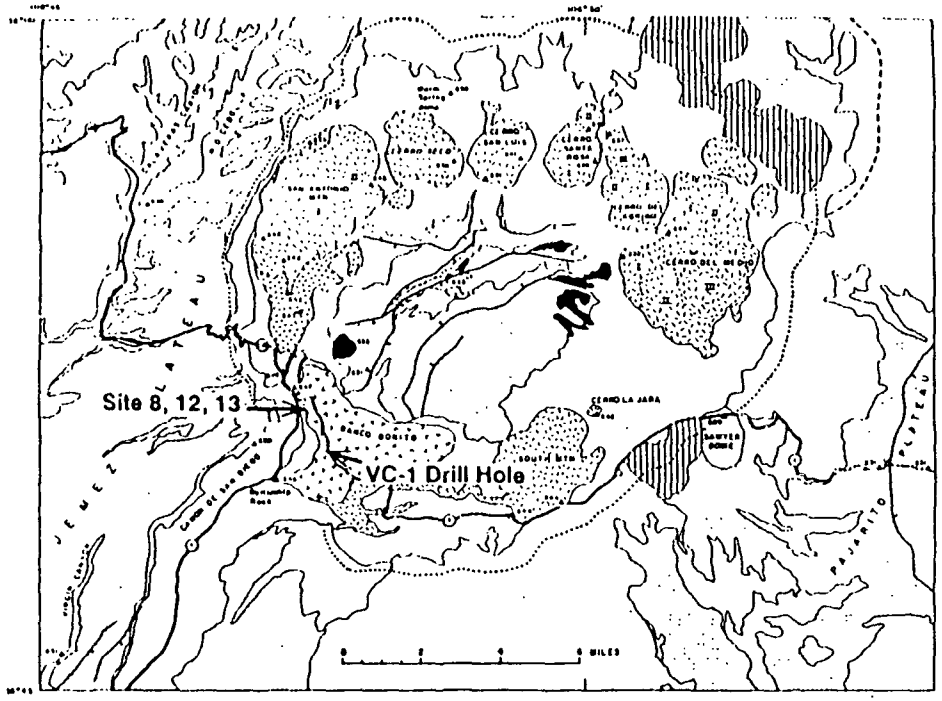

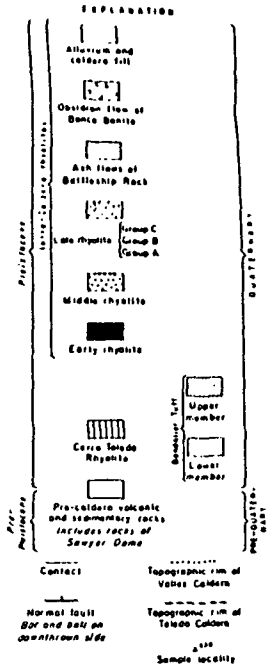

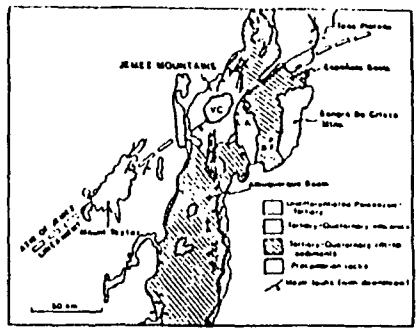

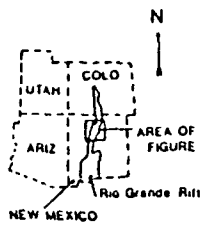

After Self et al. (1986)

GENERALIZED GEOLOGIC MAP OF VALLES CALDERA SHOWING LOCATION OF SAMPLES

VALLES CALDERA NATURAL ANALOGUE STUDY

by
H. W. Stockman and J. L. Krumhansl

Sandia National Laboratories
Geochemistry Division 6233
Albuquerque, NM

NATURAL ANALOGUE WORKSHOP
SPONSORED BY: USNRC AND CNWRA

OBJECTIVE:
Define role of natural analogue studies
in site characterization, performance assessment, and
define research priorities for geologic disposal of HLW

STRUCTURE:

FIRST PLENARY SESSION: Philosophy of Natural Analogues

WORKING GROUPS: Waste Form/Waste Package
Near-Field Processes/Environment
Far-Field Processes/Environment
Tectonics/Volcanism

SECOND PLENARY SESSION: Summaries from working groups
General discussion
Concluding Statements

PARTICIPANTS: NRC, DOE, NEVADA, Professionals from
University, Industry

NATURAL ANALOGUE FOR HOST ROCK

TIME-TEMP. CURVE FOR HIGH-LEVEL WASTE

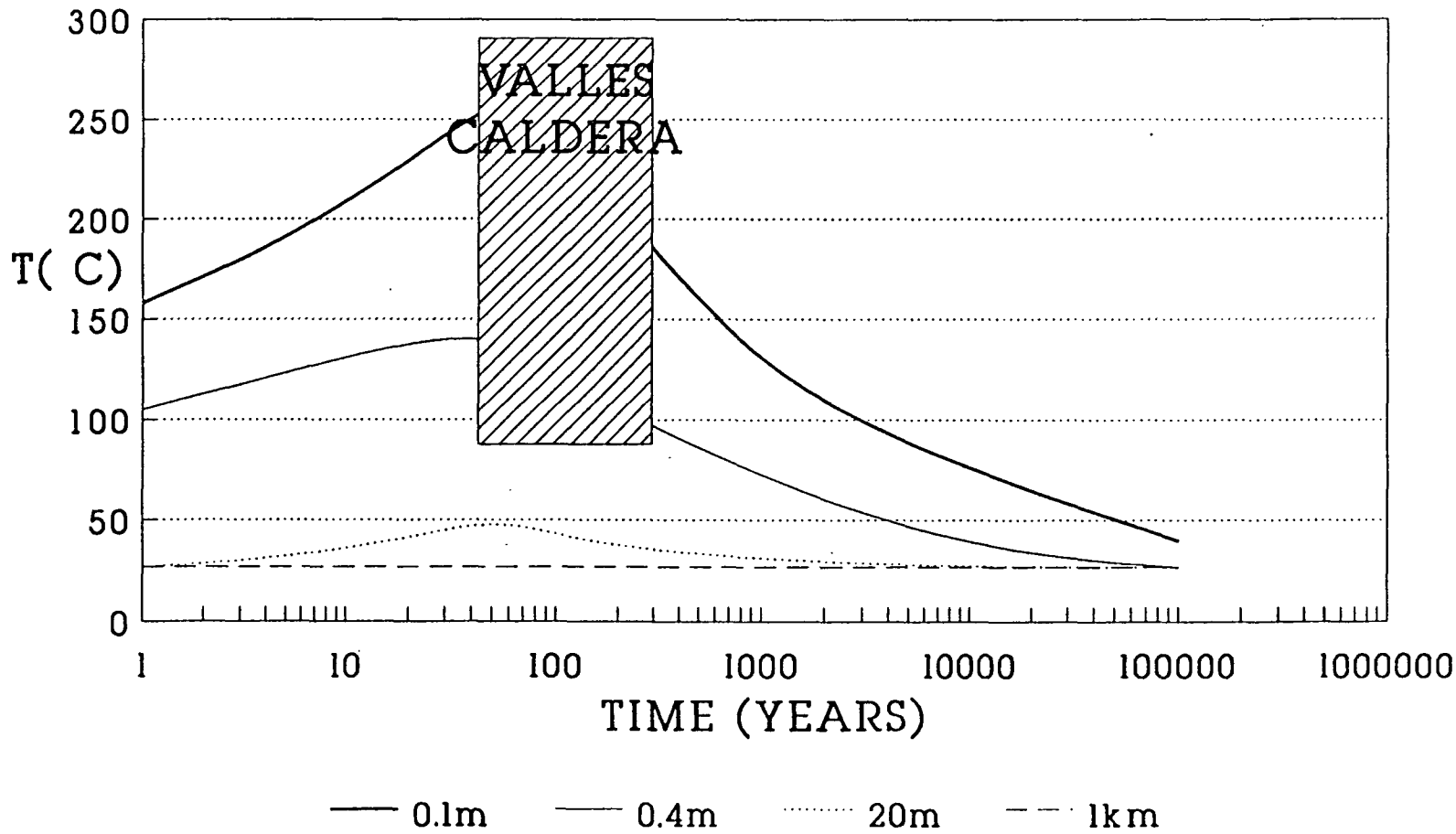

NATURAL ANALOGUE OF WASTE PACKAGE
TIME-TEMP. CURVE FOR HIGH-LEVEL WASTE

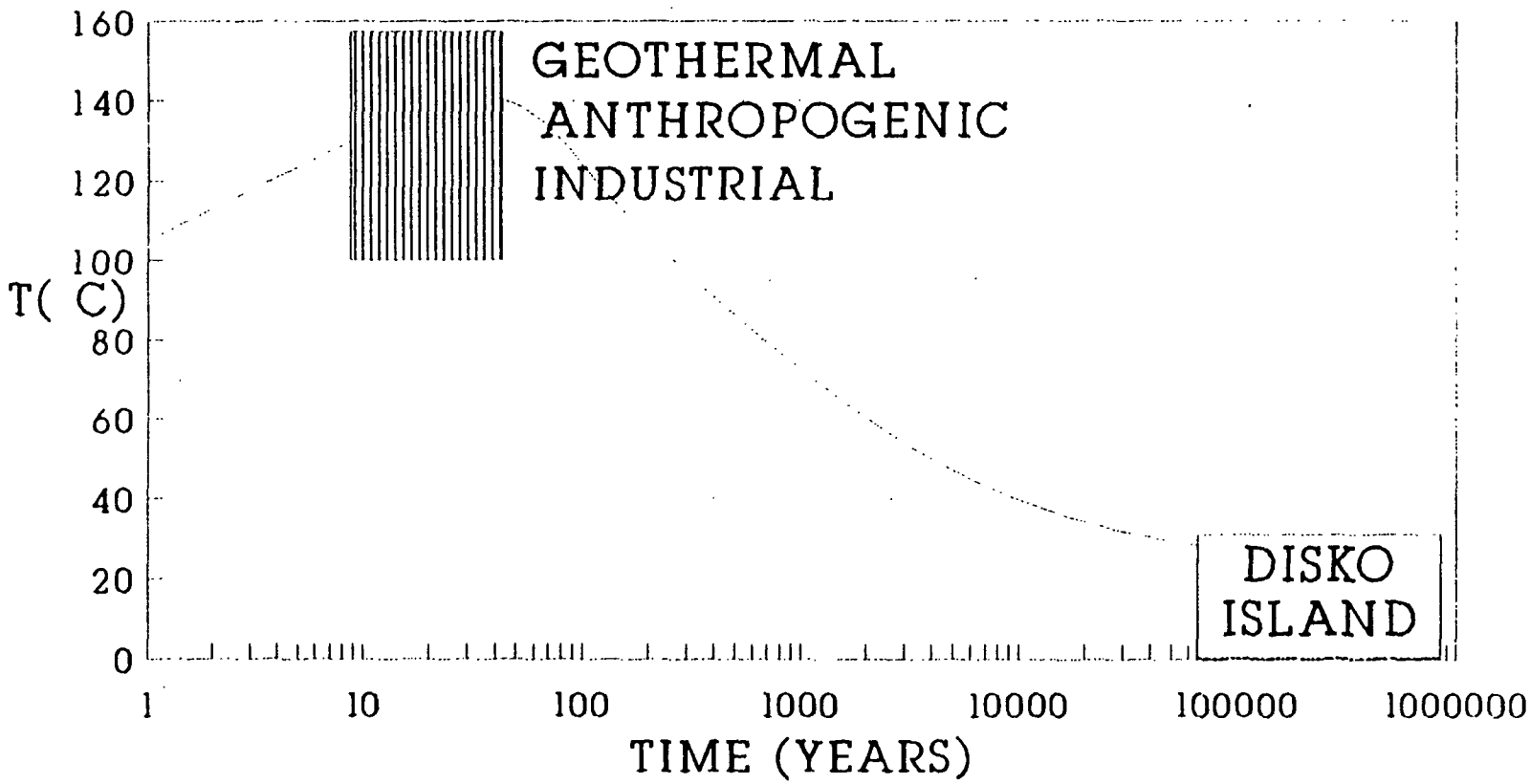

0.4m

NATURAL ANALOGUES FOR SPENT FUEL

TIME-TEMP. CURVE FOR HIGH-LEVEL WASTE

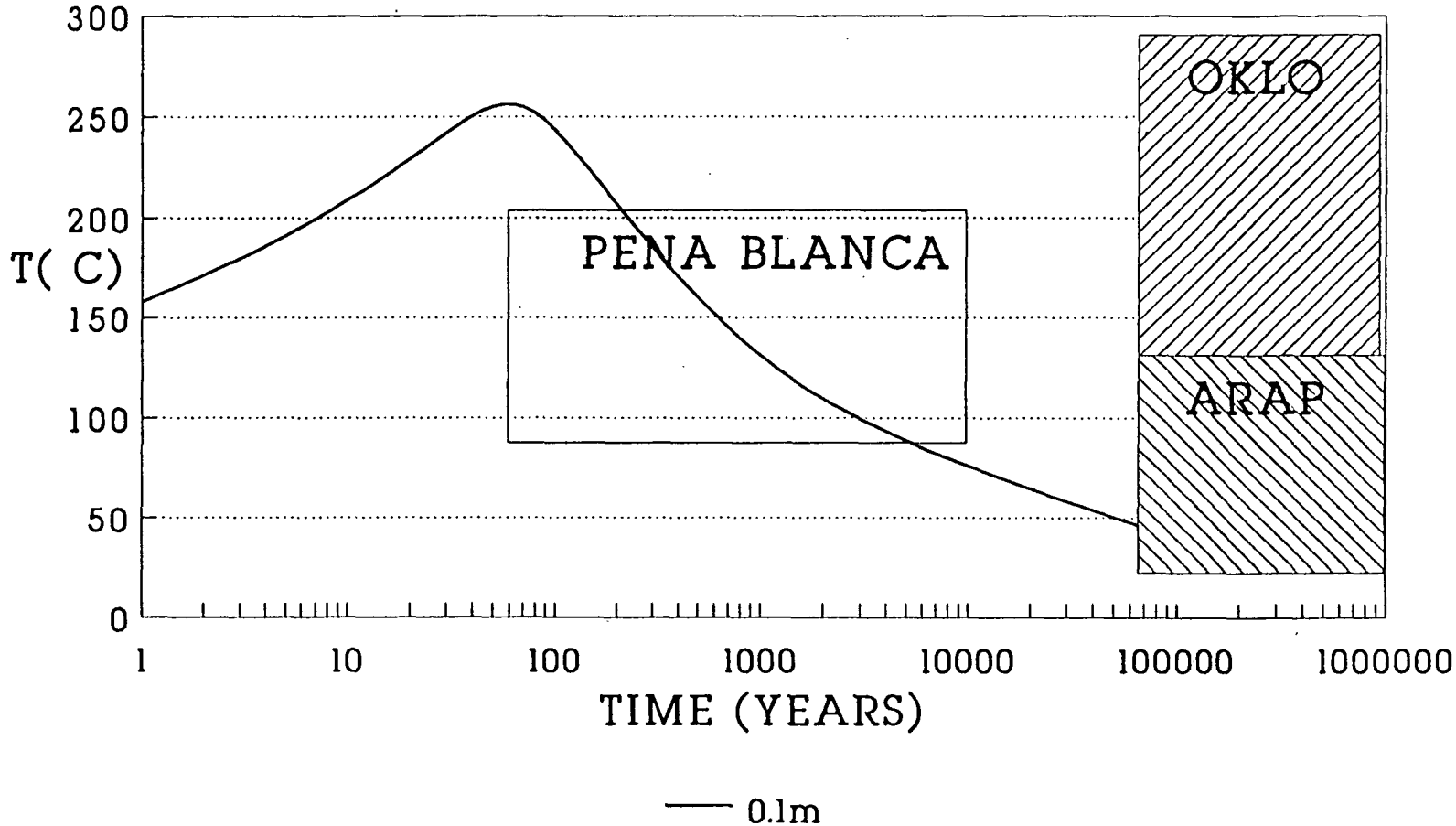

PROPOSED NATURAL ANALOGUE STUDIES

	WASTE FORM	WASTE PACKAGE	HOST ROCK STABILITY	TRANSPORT
SAT'D	OKLO McDERMITT	DISKO IS		OKLO McDERMITT
UNSAT	McDERMITT	SAN TORINI		McDERMITT SAN TORINI

CURRENT NRC NATURAL ANALOGUE STUDIES

	WASTE FORM	WASTE PACKAGE	HOST ROCK STABILITY	TRANSPORT
SAT'D	ARAP PENA BLANCA		PENA BLANCA	ARAP
UNSAT	PENA BLANCA VALLES CALDERA		VALLES CALDERA PENA BLANCA	VALLES CALDERA PENA BLANCA ARAP

ELEVATED TEMPERATURES TIME $> 10^2$ YEARS

NRC NATURAL ANALOGUE RESEARCH PLAN

FOCUS ON T - t RELATIONSHIPS

T 〉 100 C t 〉 100 - 10,000 YEARS

SUBSYSTEMS:

- WASTE FORM/WASTE PACKAGE
- HOST ROCK STABILITY
  chemical/thermal/mechanical
- HYDROGEOCHEMICAL/RADIONUCLIDE TRANSP
  UNSATURATED SYSTEMS

SCENARIO AND CONSEQUENCE ANALYSES:

- VOLCANISM/TECTONISM
- THERMOHYDROLOGY - HEAT PIPE

TIME-TEMP. CURVE FOR HIGH-LEVEL WASTE

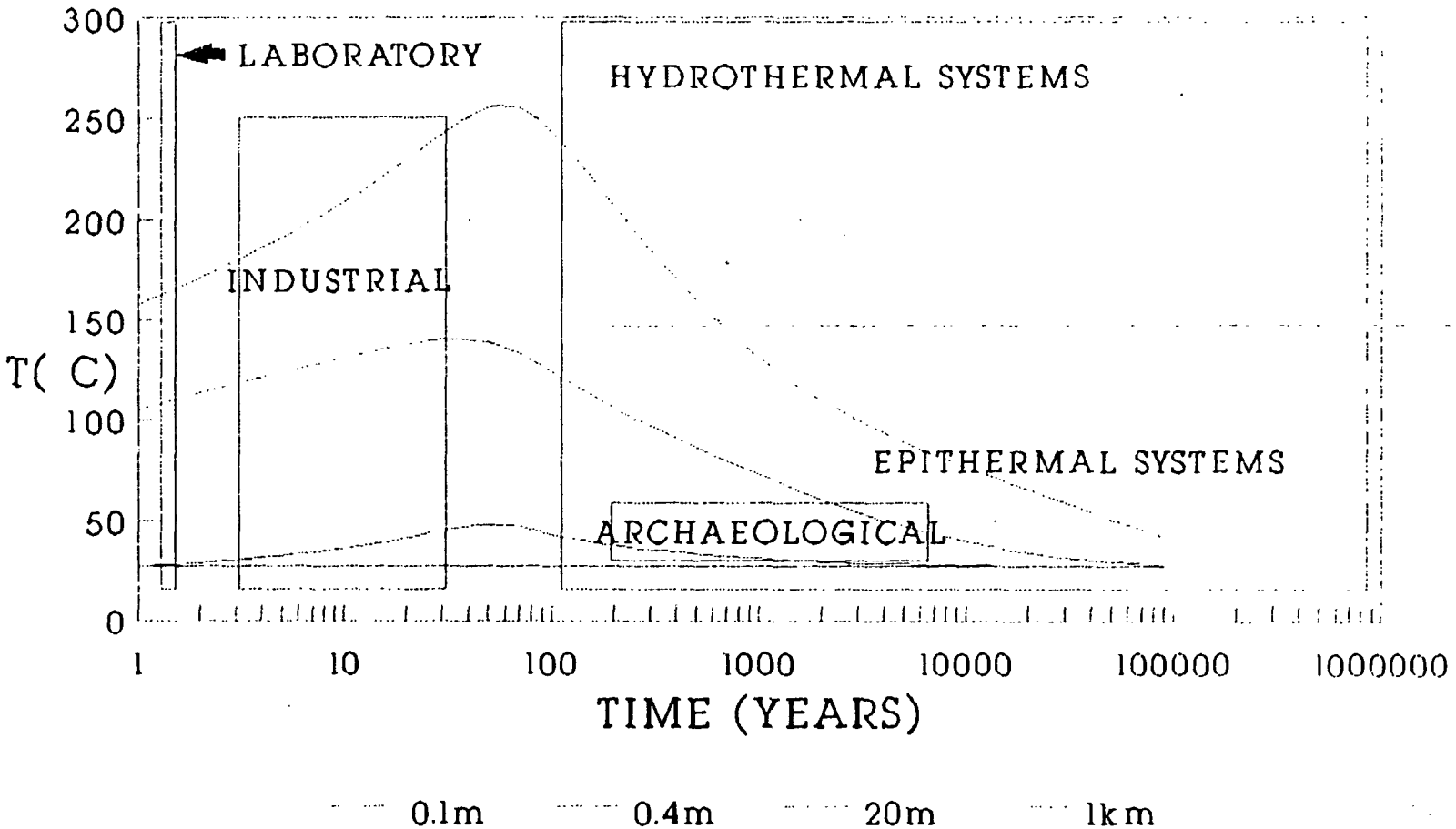

TIME-TEMPERATURE CURVE FOR HIGH-LEVEL WASTE

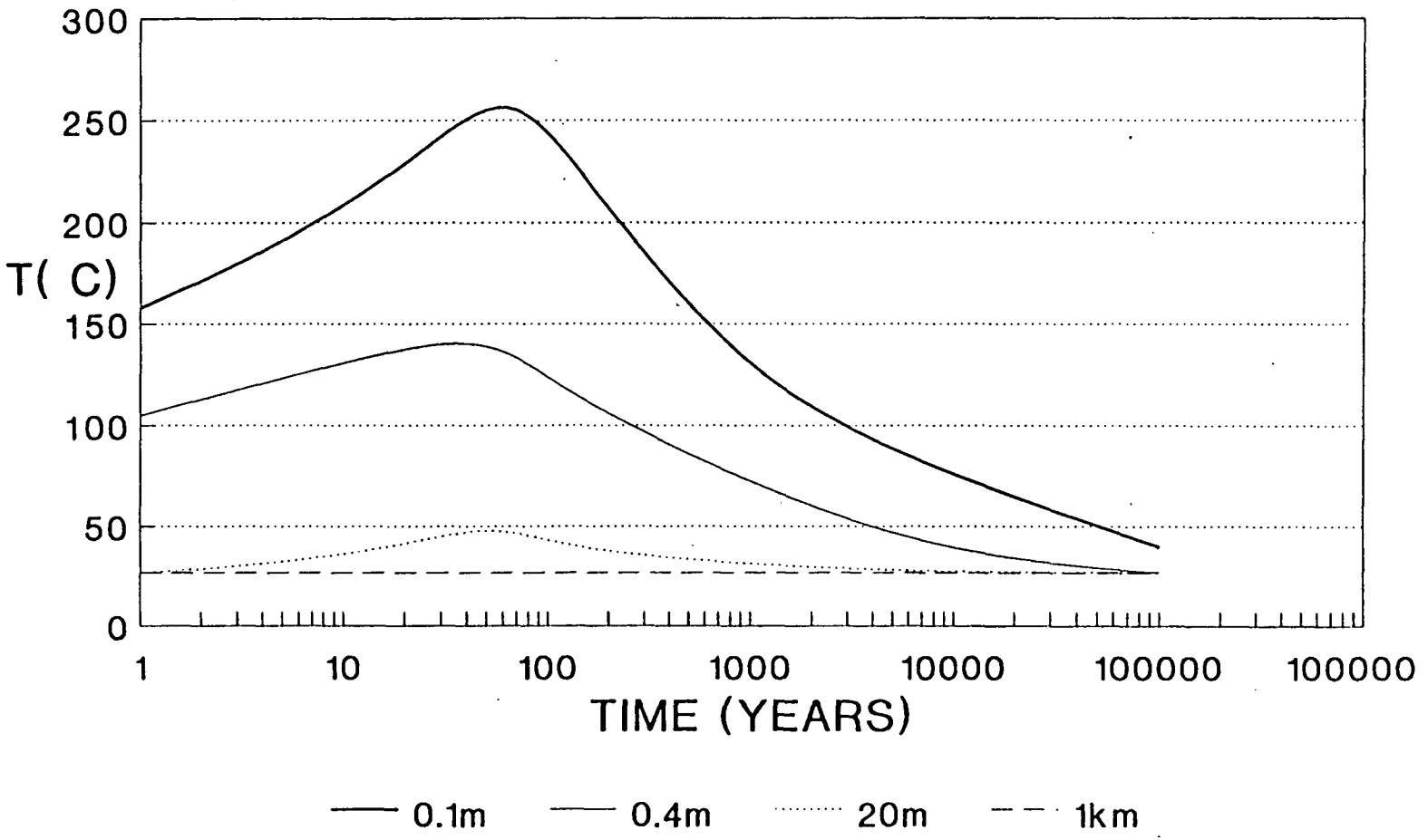

USES OF NATURAL ANALOGUES
A RESEARCH TOOL

- SCENARIO DEVELOPMENT
- SENSITIVITY STUDIES:
  Requires use of numerous analogues to bound conditions
- IDENTIFY MAGNITUDE AND EFFECTS OF COUPLED PROCESSES
- MODEL DEVELOPMENT:
  an iterative process
- DATA BASE VALIDATION:
  corroboration of experimentally or theoretically derived data
- SITE CHARACTERISATION

SELECTION CRITERIA FOR NATURAL ANALOGUES

CHAPMAN et al. (1984)

NAWG CRITERIA

- PROCESS SHOULD BE CLEAR-CUT
  other processes should be quantifiable such that effects may be subtracted
- CHEMICAL ANALOGY SHOULD BE GOOD
  limitations of chemical, mineralogical, or isotopic analogue should be fully understood
- MAGNITUDE OF PHYSICO-CHEMICAL PARAMETER (P, T, pH, Eh, CONC, etc.) SHOULD BE DETERMINABLE, preferably by independent methods
- BOUNDARY CONDITIONS OF SYSTEM SHOULD BE IDENTIFIABLE
- TIME SCALE MUST BE MEASURABLE

NATURAL ANALOGUE: A DEFINITION

THE EXISTENCE IN NATURE OF A SYSTEM ANALOGOUS TO A PROCESS OR SUBSYSTEM OF A NUCLEAR WASTE REPOSITORY

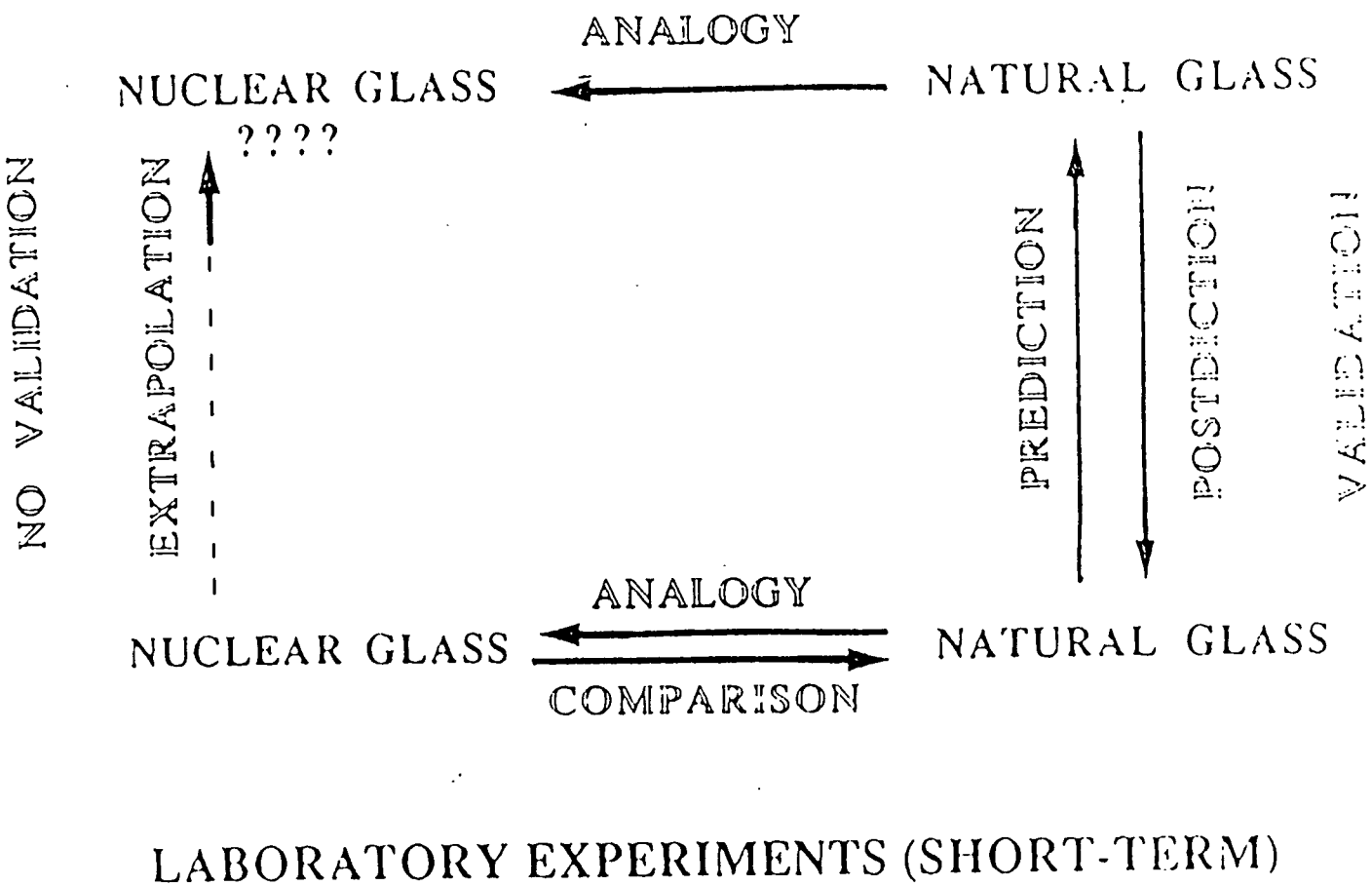

AFTER J.C. PETIT, 1990